



Research Paper

A multi-method approach to dating middle and late Quaternary high relative sea-level events on NW Svalbard – A case study

Helena Alexanderson^{a,*}, Jon Y. Landvik^a, Anatoly Molodkov^b, Andrew S. Murray^c

^a Department of Plant and Environmental Sciences, Norwegian University of Life Sciences, PO Box 5003, NO-1432 Ås, Norway

^b Research Laboratory for Quaternary Geochronology, Institute of Geology, Tallinn University of Technology, 5 Ehitajate Rd., Tallinn 19086, Estonia

^c Nordic Laboratory for Luminescence Dating, Aarhus University, Risø DTU, DK-4000 Roskilde, Denmark

ARTICLE INFO

Article history:

Received 28 June 2010

Received in revised form

28 March 2011

Accepted 1 April 2011

Available online 7 April 2011

Keywords:

Optically stimulated luminescence (OSL)

Electron spin resonance (ESR)

Radiocarbon

Sea level

Glaciations

Svalbard

ABSTRACT

Waxing and waning ice sheets and changing sea levels have been interpreted from the Quaternary stratigraphic record at Leinstranda, Brøggerhalvøya in NW Svalbard. We have identified seven high relative sea-level events, related to glacio-isostatic loading, and separated by at least four glacial events. To establish a chronology for the high sea-level events (interstadials and interglacials) and the intervening glaciations, we have used three different absolute dating methods: optically stimulated luminescence (OSL) of shallow marine deposits, and electron spin resonance (ESR) and radiocarbon (AMS-¹⁴C) dating of fossils contained in these sediments. Of the absolute dating methods, OSL has provided the stratigraphically most consistent dataset and which also matches a biostratigraphically inferred interglacial. The ESR ages of mollusc shells suffer from low precision due to unusually large uranium content in most dated shell samples, which in turn is most likely a result of significant recent uranium enrichment of the sediments. Most radiocarbon ages are non-finite. The results show that the high relative sea-level events range in age from the Saalian *sensu lato* (\geq Marine Isotope Stage, MIS, 6) to the early Holocene (MIS 1), and include events OSL-dated to 185 ± 8 ka, 129 ± 10 ka, 99 ± 8 ka and 36 ± 3 ka. The methods used by us and by previous investigators of the same site are compared and assessed, and sources of error, accuracy and precision of ages are discussed.

© 2011 Elsevier B.V. All rights reserved.

1. Introduction

Our ability to reconstruct past environments from various geological archives is improving and reconstructions are becoming more and more detailed. To place these records in a correct time frame we are dependent on absolute dating methods. Few techniques have sufficient range and capability to cover all types of deposits from the entire middle and late Quaternary and so usually a combination of methods is required. Radiocarbon dating has tended to dominate, but its age range limits the use to events younger than ~ 50 ka. For terrestrial stratigraphic studies luminescence dating is widely used, with optically stimulated luminescence (OSL) on quartz becoming a standard dating method over the last few decades. Other techniques include electron spin

resonance (ESR) and terrestrial cosmogenic nuclide (TCN) dating, both of which have a longer age range.

The choice of chronological methods depends largely on the material available. For the late Quaternary history of Svalbard, raised marine sediments and their fossil content have formed the basis for dating (Mangerud et al., 1998). Dates of the marine sediments provide the timing of comparatively ice-free intervals, when the local relative sea-level was higher than present. They also give maximum and minimum ages for under- and overlying glacial sediments. These high relative sea-level events depend partly on eustatic sea-level rise but are also related to glaciations. A locally high sea level is necessarily largely due to isostatic loading of a preceding glaciation over the archipelago or the adjacent Barents Sea shelf (Mangerud et al., 1998), since the global sea level during most of this time has been low (Waelbroeck et al., 2002).

Three major glaciations of Svalbard have been identified during the Weichselian (Marine Isotope Stage, MIS, 5d, 4, 2) and one during the Saalian (MIS 6; Mangerud et al., 1998; Svendsen et al., 2004), but there are some uncertainties regarding their exact timing and correlation across sites due to disparities between different dating methods and low chronological resolution. To

* Corresponding author. Present address: Department of Earth and Ecosystem Sciences, Lund University, Sölvegatan 12, SE-223 62 Lund, Sweden. Tel.: +46 46 2227884; fax: +46 46 2224419.

E-mail addresses: helena.alexanderson@geol.lu.se, helena.alexanderson@umb.no (H. Alexanderson), jon.landvik@umb.no (J.Y. Landvik), molodkov@gi.ee (A. Molodkov), anmu@risoe.dtu.dk (A.S. Murray).

improve our knowledge of the timing and to better understand the cause–effect relationships between ice sheets, land and sea, an accurate and precise absolute chronology of glaciations and relative sea-level change is highly desirable, not least to be able to compare the often fragmented high-resolution terrestrial record with the more continuous marine record.

Recent work at Leinstranda, Brøggerhalvøya in northwestern Svalbard has yielded more detailed information on the ice sheet dynamics during glaciations as well as relative sea-levels during interstadials/interglacials (Alexanderson et al., 2011). Here we present and discuss the chronological data from this site. Three different absolute dating methods on various materials have been used. We compare the techniques and assess the results from our study, and with those of previous investigations of the same site, and consider sources of error and other factors that may influence the accuracy and precision of the data.

2. Setting

The archipelago of Svalbard is situated in the northernmost North Atlantic between 74° and 81°N, at the boundary between cold Arctic and warmer Atlantic air- and water-masses. The focus of our studies is the Leinstranda site on Brøggerhalvøya on Spitsbergen, NW Svalbard (Fig. 1). The Brøggerhalvøya Peninsula is dominated by mainly Palaeozoic bedrock (carbonate rocks, sandstones, phyllites; Hjelle et al., 1999) with a thin Quaternary sediment cover. On central and southern Brøggerhalvøya the mountains are 500–900 m a.s.l. with several cirque and small valley glaciers, while the north-western tip is characterised by a strandflat with raised beach sediments.

The area experiences about four months of polar day and four months polar night per year. The annual air temperature at Ny Ålesund on Brøggerhalvøya (Fig. 1) is -6.3 °C and the annual

precipitation is 385 mm (average 1961–90; Norwegian Meteorological Institute). Permafrost extends to ~ 450 m depth but is shallower (~ 100 m) close to the shore, and the active layer is ~ 0.5 – 2 m thick (Orvin, 1934; Liestøl, 1976; Humlum et al., 2003; Forman et al., 2004).

The middle and late Quaternary history of Svalbard is characterised by glaciations of various extents (Mangerud et al., 1998). The terrestrial stratigraphical record is, however, largely dominated by shallow marine sediments deposited when the relative sea-level was higher than at present and not by tills (e.g. Mangerud et al., 1998; Alexanderson et al., 2011).

3. Previous studies

The Leinstranda site has previously been studied by Troitsky et al. (1979; their site 1), Miller (1982; his site 3), Miller et al. (1989; their site 15) and Forman (1999; site 15). From these studies, we have been able to identify the major units in the field and thus correlate to our stratigraphy. The investigators have used different dating methods and a summary of published ages, related to our stratigraphy (Alexanderson et al., 2011), is presented in Fig. 2. The published data include a relative chronology, with rough age inferences, based on amino acid geochronology (Miller, 1982; Miller et al., 1989) and absolute ages based on thermoluminescence (TL) dating (Troitsky et al., 1979), uranium/thorium (U/Th) dating (Miller et al., 1989) and infrared stimulated luminescence (IRSL) dating (Forman, 1999). Based on dating and/or correlation, the four high sea-level events (emergence cycles) recognised by Miller et al. (1989), have been assigned to the Saalian or older, the Eemian, the early Weichselian and the Holocene.

The more detailed stratigraphy and sedimentological analyses of Alexanderson et al. (2011) allow seven high relative sea-level

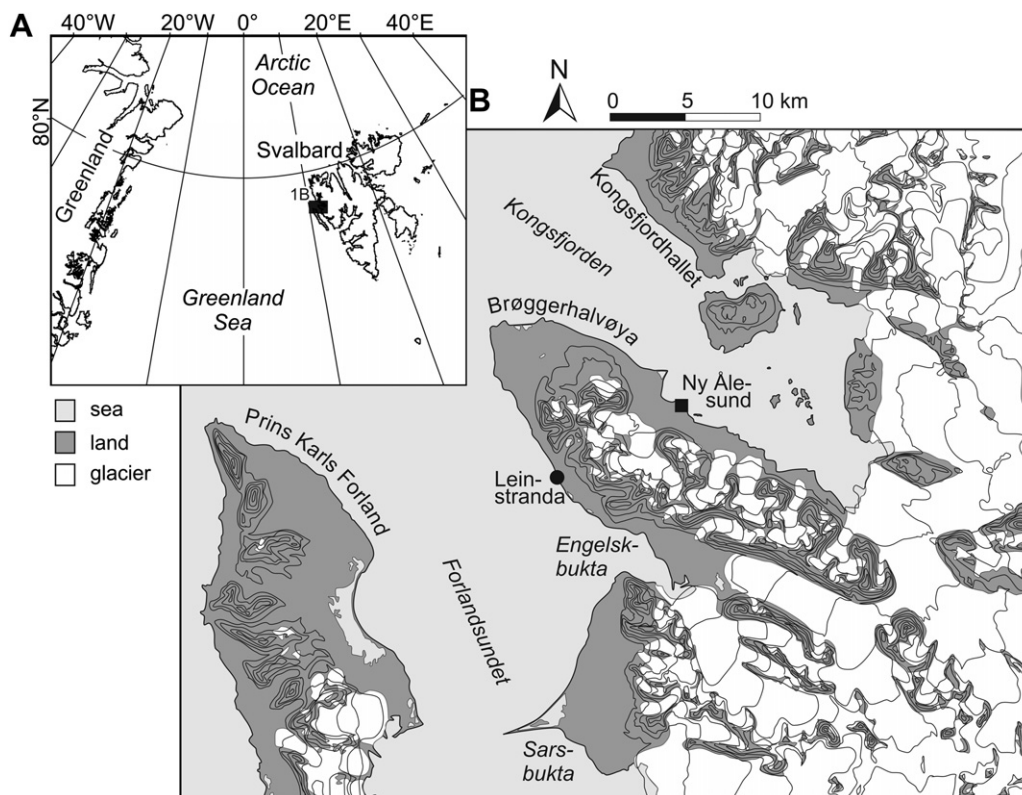


Fig. 1. (A). Location map of Svalbard in the North Atlantic, area shown in B is marked with a black square. (B). Location map of Leinstranda on the Brøggerhalvøya Peninsula, NW Spitsbergen, Svalbard. Contour interval is 100 m.

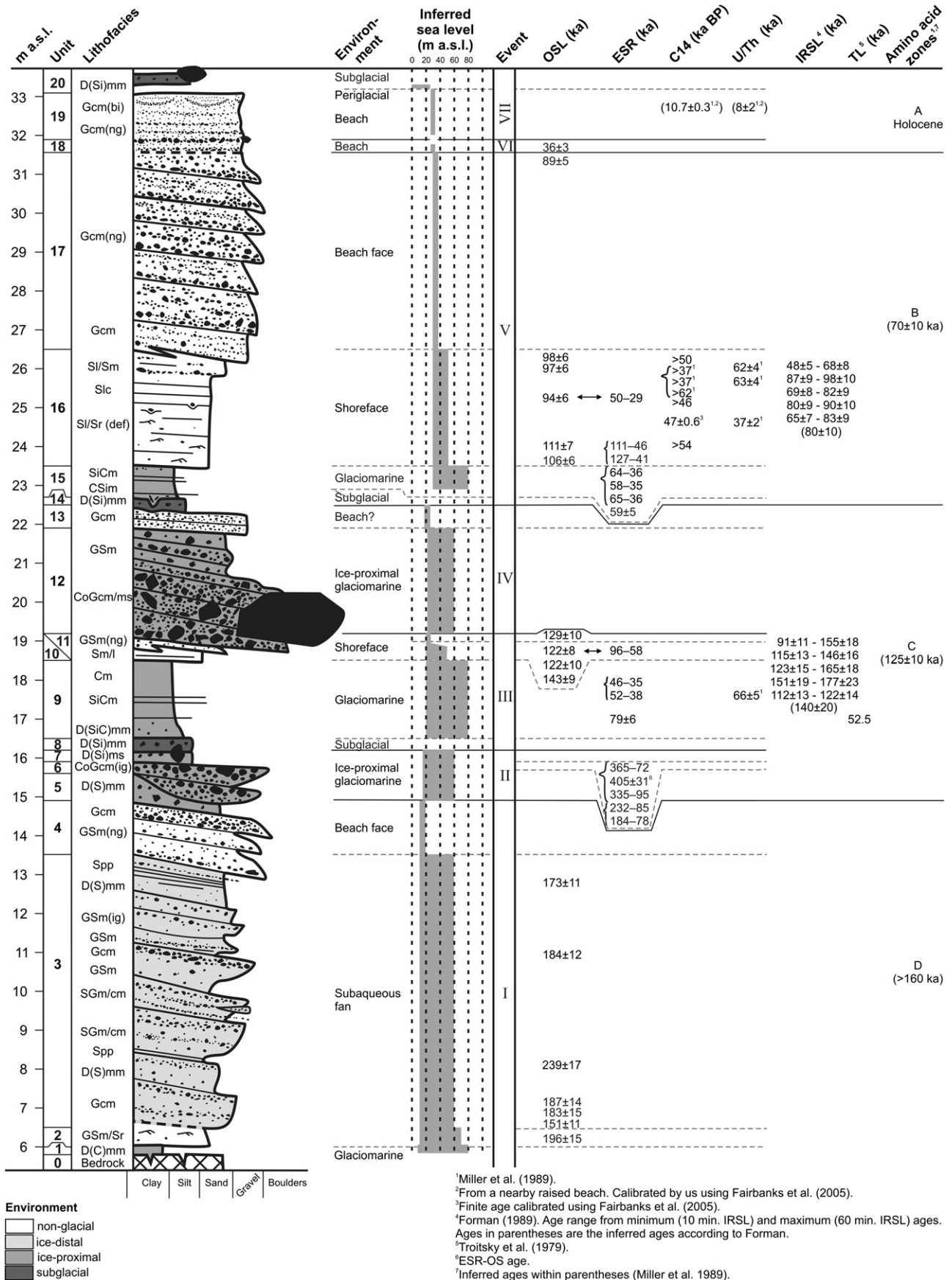


Fig. 2. Composite log of the Leinstranda section and inferred relative sea level (Alexanderson et al., 2011) with new and previously published chronological data. Parallel OSL and ESR samples are indicated by arrows. Brackets indicate samples taken from the same sampling point.

¹Miller et al. (1989).
²From a nearby raised beach. Calibrated by us using Fairbanks et al. (2005).
³Finite age calibrated using Fairbanks et al. (2005).
⁴Forman (1989). Age range from minimum (10 min. IRSL) and maximum (60 min. IRSL) ages. Ages in parentheses are the inferred ages according to Forman.
⁵Troitsky et al. (1979).
⁶ESR-OS age.
⁷Inferred ages within parentheses (Miller et al. 1989).

events to be identified (Fig. 2). They are separated by hiatuses or non-marine units, with the exception of the transitions I–II and III–IV, respectively. The latter were formed during episodes with rising sea-levels and approaching glaciers, but were not necessarily preceded by non-marine conditions at the site (cf. Alexanderson et al., 2011). The main boundaries between these events correlate well to the emergence cycle boundaries of Miller et al. (1989).

4. Methods

4.1. Field work

Field work at Leinstranda was carried out in July–August 2007, with a complementary visit in 2009. The sediments sampled for OSL include shallow marine and littoral deposits: shoreface, beachface and subaqueous fans. OSL-samples were taken in opaque plastic tubes that were hammered into sediments exposed in coastal cliffs. Next to each OSL-tube, a cylinder volumeter was inserted for measurements of water content (Pusch, 1973). In a few cases of inhomogeneous sample surroundings, an additional background sample for dose rate was taken to include any materials within a 30 cm radius of the OSL sample that were not well represented by the sampling tube. This material was later combined with material from the tube in proportion to its occurrence within a 30-cm-radius sphere centred at the sample. Background samples for ESR-analyses were taken in a similar manner while the shells for ESR dating were handpicked, as were the bones, shells and piece of wood sampled for radiocarbon dating. After sampling, all samples were stored under dark and cool conditions. Where possible, parallel samples were taken for both OSL and ESR within centimetres of each other at the same stratigraphic level; these pairs are indicated by arrows in Fig. 2.

4.2. Optically stimulated luminescence

4.2.1. Method background

Optically stimulated luminescence (OSL) dating makes use of quartz or feldspar grains to establish the time that has passed since the grains last were exposed to daylight, i.e. when they were deposited. Electrons become trapped within the mineral crystals following ionisation by natural radiation during burial; by determining the number of trapped electrons (as luminescence) and the amount of energy absorbed from radiation per time unit, the time

since burial can be calculated (e.g. Aitken, 1998). Over the last 20 years the method has been frequently and successfully used to date late Quaternary deposits of various kinds (e.g. Duller, 2004; Lian and Roberts, 2006), including high-latitude modern and Pleistocene marine and glaciomarine deposits, e.g. Mangerud et al. (1998) and Forman (1999) on Svalbard, and Jakobsen et al. (2003); Kjær et al. (2003, 2006); Berger (2006) and Möller et al. (2008) elsewhere in the Arctic. Its usefulness is, however, partly dependent on geological setting (characteristics of the analysed mineral, cf. Alexanderson and Murray, in press) and on type of deposit (e.g. risk of incomplete bleaching). Jacobs (2008) has recently provided a comprehensive review of luminescence dating in marine and coastal environments.

4.2.2. Sample preparation

The preparation of OSL-samples was done at the Norwegian University of Life Sciences (mechanical preparation) and at the Nordic Laboratory for Luminescence dating (chemical preparation and measurement). The sample tubes were opened under subdued red light and the outer ~4 cm from each end were used for dose rate measurements (subsample 1), while the central part was used for dose measurements (subsample 2). Subsample 1, if necessary complemented by additional material (see above), was dried, weighed, heated to 450 °C for loss on ignition, weighed again and then crushed to approximately fine sand – silt size before being mixed with wax and cast into cups for gamma spectrometry measurements.

Subsample 2 was wet-sieved and the fraction 180–250 µm was chosen for further analyses. After treatment with 10% HCl to remove carbonates (5–120 min, depending on carbonate content) and 10% H₂O₂ to remove organic material (15 min), the selected fraction of subsample 2 was density separated using lithium heteropolytungstate (LST) heavy liquid at 2.62 g/cm³. The lighter separate, consisting mainly of feldspars, was archived while the heavier one was etched with 38% HF for 1 h, followed by 10% HCl for 40 min. After drying, it was tested for purity with an IR-test (cf. Duller, 2003) and then measured.

4.2.3. Measurements

The cylinder volumeters were weighed with natural water content, saturated (after 24 h covered by water) and dried (after at least 24 h at 105 °C) and the natural and saturated water contents were calculated as weight% (Pusch, 1973). The activity of

Table 1

Summary of radionuclide specific activities measured with high-resolution gamma spectrometry on the OSL samples from Leinstranda. Beta and gamma dose rates refer to dry material; for water contents and final dose rates see Table 3.

Sample	²³⁸ U (Bq/kg)	²²⁶ Ra (Bq/kg)	²³² Th (Bq/kg)	⁴⁰ K (Bq/kg)	Beta (Gy/ka)	Gamma (Gy/ka)
081323	20 ± 4	16.8 ± 0.4	5.7 ± 0.3	124 ± 4	0.51 ± 0.02	0.29 ± 0.01
081324	16 ± 6	21.0 ± 0.5	9.1 ± 0.5	155 ± 6	0.61 ± 0.03	0.38 ± 0.02
081325	15 ± 4	19.3 ± 0.4	15.4 ± 0.4	245 ± 6	0.86 ± 0.02	0.52 ± 0.02
081326	28 ± 5	17.4 ± 0.4	19.1 ± 0.5	341 ± 8	1.17 ± 0.03	0.63 ± 0.02
081327	20 ± 4	16.7 ± 0.4	17.6 ± 0.4	275 ± 7	0.96 ± 0.03	0.56 ± 0.02
081328	24 ± 8	20.4 ± 0.7	9.1 ± 0.7	153 ± 8	0.60 ± 0.04	0.33 ± 0.02
081329	16 ± 4	15.9 ± 0.3	10.7 ± 0.3	194 ± 5	0.69 ± 0.02	0.40 ± 0.01
081330	12 ± 9	20.4 ± 0.7	12.5 ± 0.7	217 ± 9	0.77 ± 0.04	0.47 ± 0.02
081331	21 ± 4	21.8 ± 0.4	10.3 ± 0.4	117 ± 5	0.55 ± 0.02	0.38 ± 0.02
081332	18 ± 4	21.0 ± 0.4	5.6 ± 0.3	111 ± 4	0.49 ± 0.02	0.31 ± 0.02
081333	18 ± 6	15.3 ± 0.5	17.0 ± 0.6	292 ± 9	0.98 ± 0.03	0.55 ± 0.02
081334	19 ± 4	18.3 ± 0.3	15.5 ± 0.3	240 ± 5	0.86 ± 0.02	0.51 ± 0.02
081335	13 ± 2	15.8 ± 0.2	12.8 ± 0.2	208 ± 4	0.73 ± 0.02	0.43 ± 0.01
081336	17 ± 2	19.0 ± 0.3	8.6 ± 0.2	149 ± 3	0.59 ± 0.02	0.36 ± 0.02
081337	26 ± 7	23.9 ± 0.6	9.4 ± 0.5	132 ± 6	0.62 ± 0.03	0.39 ± 0.02
081338	15 ± 3	13.9 ± 0.3	6.1 ± 0.2	111 ± 3	0.44 ± 0.02	0.26 ± 0.01
081339	2 ± 8	22.3 ± 0.6	7.9 ± 0.6	173 ± 7	0.60 ± 0.04	0.39 ± 0.02
081340	22 ± 5	22.7 ± 0.5	6.3 ± 0.4	101 ± 5	0.50 ± 0.03	0.32 ± 0.02

radionuclides in the sediment was determined with high-resolution laboratory-based gamma spectrometry (Table 1; Murray et al., 1987).

The luminescence was measured from large aliquots of quartz on Risø TL/OSL-readers equipped with calibrated $^{90}\text{Sr}/^{90}\text{Y}$ beta radiation sources (dose rate 0.05–0.27 Gy/s), blue (470 ± 30 nm; ~ 50 mW/cm²) light sources, and detection was through 7 mm of U340 glass filter (Bøtter-Jensen et al., 2000). Each aliquot contained about 1500–2000 grains. Analyses were carried out using single aliquot regenerative (SAR) protocols (Table 2) (Murray and Wintle, 2000, 2003). Dose measurements at different preheat/cutheat combinations (preheat plateau tests) show that the dose, within errors, is largely independent of temperatures up to 260 °C (Fig. 3). Higher temperatures give apparently higher doses, which may be due to thermal transfer. The chosen temperature combination for the majority of the samples (220°/180°) is situated on the middle of the plateau and gave good recycling ratios and low recuperation. The quartz is bright, with a signal dominated by the fast component (Fig. 4A). In four samples, an ultrafast signal component was also detected; the importance of this was minimised by using higher preheat and cutheat temperatures (protocol B, Table 2; cf. Jain et al., 2008). IR-tests showed that the infrared stimulated signal (from feldspar) was small in relation to the blue stimulated signal (from quartz) for all samples (generally <3%), and any feldspar contamination was therefore deemed insignificant.

At least 20, usually 24 aliquots were measured for each sample but for a few samples the amount of material set lower limits. Extended growth curves show that the luminescence response to dose continues to rise well above the natural equivalent doses and the samples do not appear to be close to saturation (Fig. 4B). A typical D_0 for the Leinstranda samples is ~ 110 Gy, suggesting that the maximum measurable dose is in the order of ~ 220 Gy, above the observed D_e 's (Table 3).

Dose recovery tests were carried out for at least 3 aliquots per sample, sometimes more. Bleaching for dose recovery tests was done with a Hönle SOL2 solar simulator for 1 h. The dose recovery results for all aliquots that passed the rejection criteria and that were measured with the appropriate protocol averages 1.02 ± 0.03 ($n = 52$; given dose range 31–120 Gy; Fig. 5) which demonstrates that the selected protocols are able to recover a dose given in the laboratory before any heat treatment. The mean recycling ratio for all accepted dose recovery measurements is 0.969 ± 0.009 ($n = 52$) and for all dose estimates 0.998 ± 0.003 ($n = 434$). Recuperation is generally small.

4.2.4. Data analysis

Equivalent doses were calculated using Risø Analyst 3.24 with exponential curve fitting (Table 3). The first 0.8 s (channels 1–5 of

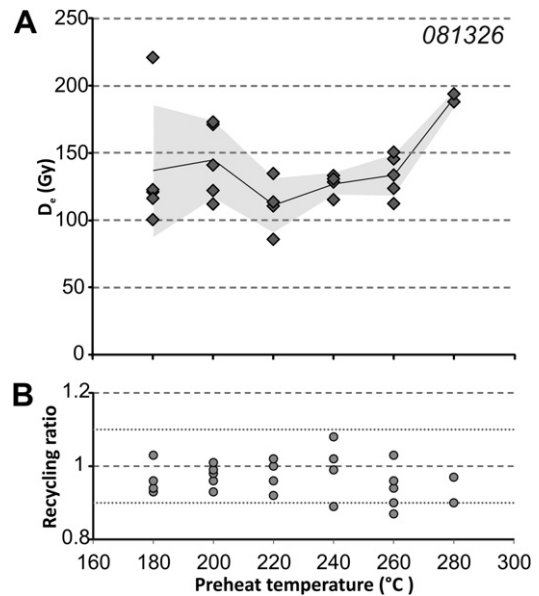


Fig. 3. A. Preheat plateau for sample 081326 from unit 16; cutheat was 40 °C lower than the preheat. An increased dose, possibly due to thermal transfer, is evident for the highest temperature combination. However, there are also some high-dose outliers for low temperatures. The shaded area with the full line is the standard deviation and the mean D_e of the aliquots for each temperature. B. Recycling ratios for the same aliquots; the hatched lines represent 10% range from unity.

250) were used for peak integration and the following 0.8 s (channels 6–10) for background (cf. Cunningham and Wallinga, 2010). For the young sample 081341 channels 1–10 and 11–20 were used to improve counting statistics. Aliquots were rejected if the recycling ratio was more than 10% from unity, test dose error >10%, equivalent dose error >50% or the signal less than three sigma above the background. However, only few aliquots had to be rejected (Table 3). Signal component analyses were done in SigmaPlot 10.0 using the formulae of Choi et al. (2006). The final ages were calculated as the mean of the accepted aliquots, with the standard error representing the uncertainty associated with each age. As a comparison, ages were also calculated according to the minimum-age model (Galbraith et al., 1999; excel macro developed by Sébastien Huot), after adding an overdispersion value of 15%.

The total dose rate was calculated from the gamma spectrometry data (Tables 1 and 3), assuming secular equilibrium and using the dose-rate conversion factors of Adamic and Aitken (1998), with the addition of cosmic rays (Prescott and Hutton, 1994), and assuming a water content close to saturation. The water content was estimated by using the saturated value (range 27–35%) for 95% of the time since deposition, and the current (at sampling) water content (range 3–18%) for 5% of the time. This assumption is based on that the sediments for most of the time since deposition have been at or close to saturation, because of being below sea-level, below a glacier with basal melting or within the permafrost zone. No indications of past or present large ground ice bodies have been found at the site and the pore-space ice content is therefore believed to be roughly similar to the water content.

4.3. Electron spin resonance

4.3.1. Method background

Since Ikeya and Ohmura (1981) first recognised mollusc shell material as a possible dating object by electron spin resonance, the method has been gradually improved (e.g. Molodkov, 1988, 1993)

Table 2
Summary of the settings for the three different SAR-protocols used for measurement of the Leinstranda OSL-samples.

Step	Procedure	A ^a	B ^b	C ^c
1	Give dose (except for first run)			
2	Preheat	220 °C	260 °C	180 °C
3	Optically stimulate with blue LEDs for 40 s at 125 °C			
4	Give test dose	17–34 Gy	20–27 Gy	2–7 Gy
5	Heat (thermoluminescence)	180 °C	240°	160 °C
6	Optically stimulate with blue LEDs for 40 s at 125 °C			
7	Illuminate with blue LEDs for 40 s at 280 °C			
8	Return to 1			

^a All samples except those listed for protocols B and C.

^b Samples 081334, 35, 37, 39.

^c Sample 081341.

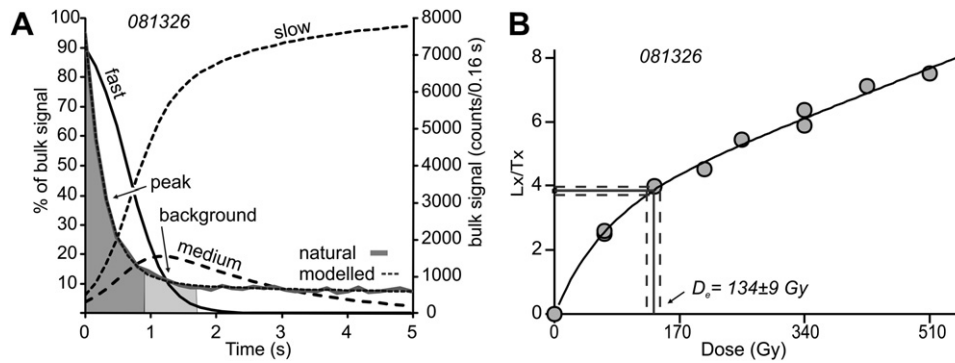


Fig. 4. (A). A natural decay curve and signal components (fast, medium, slow; cf. Bailey et al., 1997) for sample 081326 from unit 16 during the first 5 s (of total 40 s) illumination. The shaded areas indicate the peak and background integration intervals, respectively. The simple component analysis of the continuous wave OSL data was made according to the formulae of Choi et al. (2006). (B). An extended growth curve of the same sample and aliquot as in A shows that the luminescence response continues to grow with increased dose and, thus, that the sample does not become saturated within the dose range of these samples.

and has become a most useful chronostratigraphic tool for the early Pleistocene to the late Holocene (Grün, 1989; Rink, 1997). The ESR method has successfully been applied to shell-bearing deposits of marine, freshwater and terrestrial genesis (e.g. Schellmann and Radtke, 1997; Molodkov, 2001; Molodkov et al., 2002; Molodkov and Bolikhovskaya, 2002, 2009).

The method is based on direct measurement of the amount of radiation-induced paramagnetic centres, formed in shell material exposed to natural radiation. At the time of formation, the lattice of biogenic carbonate in the shell has no radiation-induced centres, but ionising radiation from the shell itself and the environment (including matrix and cosmic) causes their gradual accumulation. A shell sample will therefore have long-lived ($\sim 10^7$ – 10^9 years at -6 °C, Molodkov, 1988, 1989) paramagnetic centres, the number of which relates directly to the total radiation dose that the shell has received, and so to the age of the shell and of the enclosing sediments. The presence and number of paramagnetic carbonate centres in mollusc shell material are detected by ESR spectrometry, which produces a plot of the microwave absorption derivative spectrum (Fig. 6) where each paramagnetic centre is characterised by a specific signal (line). The amplitude of this signal is related to the accumulated palaeodose (equivalent dose), and hence to the age of the shells. The position of an ESR

line in a spectrum is described by the g -value, which characterises the type of the paramagnetic centre. Potential sources of error are, e.g., related to open system behaviour of the uranium series, thermal instability of the signal and inflection points in the growth curves (Katzenberger and Willems, 1988; Grün, 1991; McLaren and Rowe, 1996).

4.3.2. Sample preparation

The ESR method has been applied in the present study to date marine mollusc shells (species of *Mya truncata*, *Hiatella arctica* and *Astarte* sp.) taken directly from the section of the Leinstranda site. Single whole valves and in some cases paired valves were used.

The shells were washed in distilled water; the remnant sand and clay minerals were removed in an ultrasonic bath; shell thickness was measured and they were etched by diluted acetic acid in order to remove 20 μm of the alpha-irradiated surface from either side of the shell, then washed repeatedly in distilled water and dried at room temperature. The dried shell samples were gently ground with an agate mortar and pestle, sieved in order to separate the fraction of 70–400 μm , washed four times with distilled water to remove adhered <70 μm particles, then allowed to dry at room temperature again.

Finally each sample was normally divided into 11 aliquots. Of those 10 were irradiated by a calibrated ^{60}Co source with a dose

Table 3

OSL doses and ages presented in stratigraphic order. The uncertainty of each event age is the standard deviation of the population of mean sample ages. OD is overdispersion.

Sample no.	Unit	Deposit type	Depth (m)	MAM3 age ^a (ka)	Mean age (ka)	Dose (Gy)	OD (%)	Skewness	n	Dose rate (Gy/ka)	w.c. (%)	Inferred age (ka) of event
081341	—	beach	0	—	—	0.24 ± 0.05	23	−0.32	15 (18)	—	—	
081323	18	beachface	1.5	30 ± 3	36 ± 3	29 ± 2	30	2.04	26 (27)	0.80 ± 0.04	31	VI: 36 ± 3
081333	17	beachface	2.8	87 ± 5	89 ± 5	113 ± 3	14	0.17	25 (27)	1.27 ± 0.05	33	V: 99 ± 8 MIS 5c
081324	16	shoreface	7.0	96 ± 9	98 ± 6	87 ± 2	11	0.13	25 (26)	0.89 ± 0.05	26	
081325	16	shoreface	7.3	93 ± 6	97 ± 6	108 ± 5	17	2.42	25 (26)	1.11 ± 0.05	33	
081326	16	shoreface	8.0	88 ± 6	94 ± 6	131 ± 5	18	1.59	28 (28)	1.40 ± 0.06	33	
081327	16	shoreface	9.5	109 ± 6	111 ± 7	132 ± 5	14	0.76	23 (24)	1.18 ± 0.05	33	
081334	16	shoreface	9.0	104 ± 6	106 ± 6	120 ± 4	9	0.53	24 (24)	1.13 ± 0.05	28	
081328	11	beachface	14.0	123 ± 9	129 ± 10	98 ± 4	18	2.01	23 (24)	0.76 ± 0.05	32	III: 129 ± 10 MIS 5e
081329	10	shoreface	14.5	121 ± 8	122 ± 8	116 ± 4	12	0.96	23 (24)	0.94 ± 0.05	22	
081330	10	shoreface	14.5	113 ± 8	122 ± 10	121 ± 7	23	−0.51	23 (24)	0.99 ± 0.05	30	
081335	10	shoreface	14.5	135 ± 9	143 ± 9	134 ± 5	16	1.62	24 (24)	0.94 ± 0.04	30	
081331	3	subaqueous fan	20.5	172 ± 12	173 ± 11	133 ± 3	10	−0.43	22 (24)	0.77 ± 0.04	28	I: 185 ± 8 MIS 7/6
081336	3	subaqueous fan	22.5	182 ± 12	184 ± 12	141 ± 5	10	1.14	18 (20)	0.77 ± 0.04	30	
081332	3	subaqueous fan	25.0	237 ± 18	239 ± 17	156 ± 5	9	1.49	17 (20)	0.65 ± 0.04	30	
081337	3	subaqueous fan	26.0	183 ± 13	187 ± 14	151 ± 6	17	1.11	24 (24)	0.81 ± 0.05	29	
081338	3	subaqueous fan	26.5	172 ± 13	183 ± 15	109 ± 5	17	2.11	24 (24)	0.60 ± 0.04	28	
081339	3	subaqueous fan	26.8	149 ± 11	151 ± 11	119 ± 3	12	1.21	24 (24)	0.79 ± 0.05	30	
081340	2	shoreface	27.0	193 ± 14	196 ± 15	128 ± 4	17	0.42	27 (27)	0.65 ± 0.04	32	

^a Ages calculated by the three-parameter Minimum Age Model (Galbraith et al., 1999, excel macro by Sébastien Huot).

^b Excludes two outliers for reasons discussed in text.

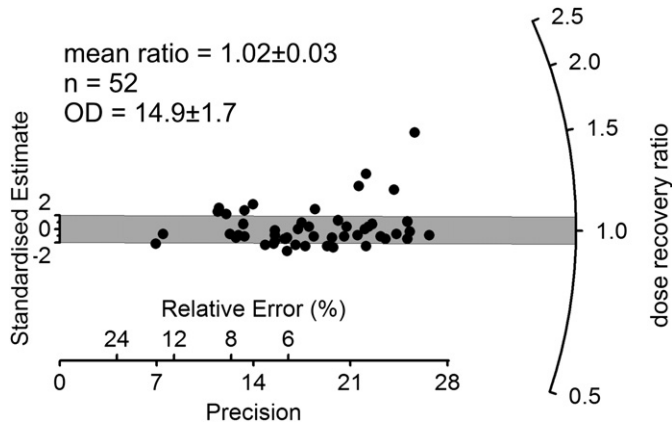


Fig. 5. Radial plot of dose recovery results for all accepted aliquots measured with the chosen protocols, cf. Table 2. The mean ratio is close to one which shows that our protocols are able to recover a given dose. Three of the higher outliers are from the same sample, 081327, indicating that the equivalent doses from that sample may be slightly overestimated.

rate of about 47 mGy s^{-1} at doses ranging from 100 to 1000 Gy with radiation steps of 100 Gy. After irradiation, all shell aliquots were annealed for 2 h at 100°C to allow fading of any possible short-lived ESR signals induced by laboratory radiation.

4.3.3. ESR analysis

All ESR age determinations were carried out at the Research Laboratory for Quaternary Geochronology (RLQG), Institute of

Geology, Tallinn University of Technology. An overview of the ESR dating procedure used in RLQG is presented in Molodkov et al. (1998). A brief outline of the procedure is given below.

Shell samples were analysed with an ESR-221 spectrometer (X-band) at room temperature. All the shells studied were composed of aragonite, and displayed typical ESR spectra (Fig. 6). Quantification of the 2.0012 centre (Molodkov, 1988) concentration was obtained from the peak-to-peak amplitude in derivative over-modulated spectra of the shell. The over-modulation (OM) detection technique (Molodkov, 1988, 1993) was used to enhance the analytical line at $g = 2.0012$, $\Delta B_{pp} \approx 0.22 \text{ mT}$ (measured with magnetic field modulation of 0.025 mT), and to suppress the narrower interfering radiation-induced signals at g_1 – g_4 and broader signal at g_5 (Fig. 6) minimising superposition effects from these lines. The method applied assures dosimetric read-out of the intensity of the true resonance line shape, which is a more precise parameter compared to the overlapping peak intensities of the high-resolution ESR derivative spectra traditionally employed. The line at $g = 2.0012$ was recorded with a sweep width of 100 mT , a scan speed of 3.7 mT/min , and time constant of 0.01 s . The microwave power used for these measurements was 2 mW with 100 kHz magnetic field modulation at 1 mT .

Reconstruction of palaeodose, P , was performed by extrapolating the regression lines to zero ESR intensities. The multiple-aliquot additive-dose technique was applied to construct dose-dependent curves. The data points used for ESR regression are the means of up to ten measurements of the $g = 2.0012$ ESR signal (Molodkov, 1988, 1993) for each aliquot. The range of correlation coefficients (R^2) varied from about 0.999 to 0.9999 for all samples, which indicates the reliability of the determination of the key

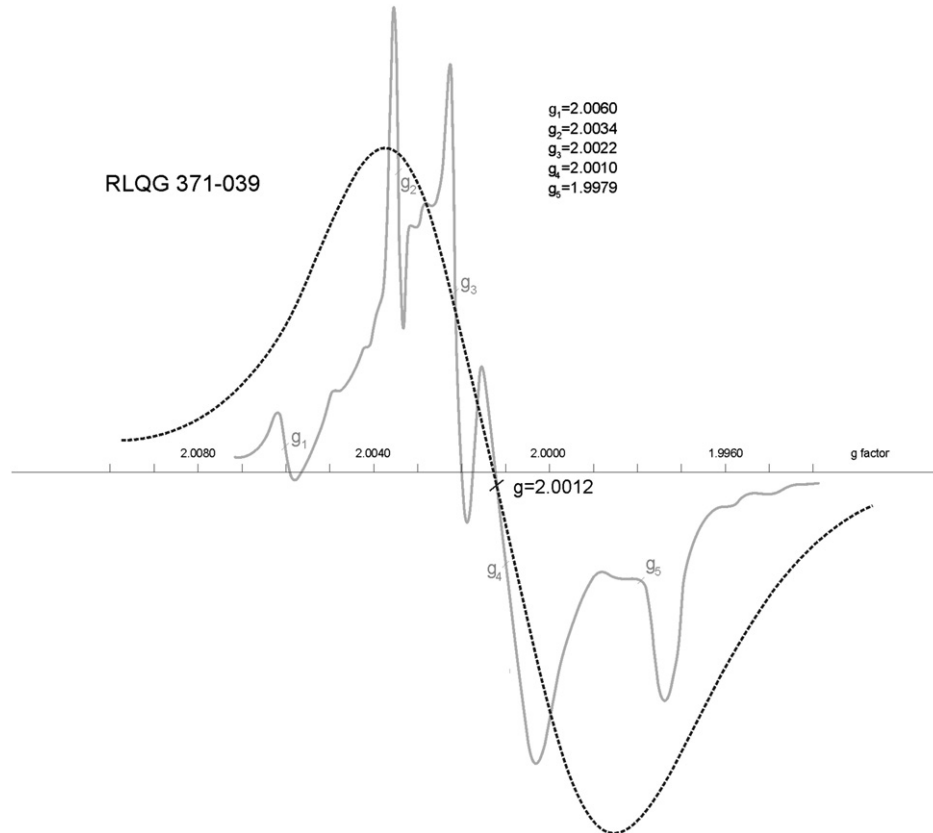


Fig. 6. Typical ESR spectra of the shell samples from the Leinstranda site. The analytical signal at $g = 2.0012$ (dotted) is extracted from the conventional shell spectrum (solid) by modulation amplitude of 1 mT (over-modulation (OM) detection method; Molodkov, 1988, 1993). The OM-signal intensity is normalised with respect to the peak intensities of the conventional ESR spectra of the shell recorded at much smaller modulation amplitude of 0.025 mT .

parameter of radiation exposure dating methods – the accumulated palaeodose, P (Fig. 7).

External dose determination is broadly similar to that for OSL dating (see above). Internal dose rate was calculated based on the determination of U-content in the shells by ICP-MS, taking into account the in-growth of ^{230}Th with daughters in the shell during its buried state (Ikeya, 1985; Molodkov, 1986; Molodkov et al., 1998). However, mollusc shell may act as an open system in regard to uranium (McLaren and Rowe, 1996), which may, in the case of considerable uranium enrichment in the shells, lead to appreciable uncertainties in the determination of the internal dose rate of the shells. Therefore, an ESR open system (ESR-OS) dating method (Molodkov, 1988) should be applied in this case. In the present study we have used this method, based on thermal ionisation mass spectrometry (TIMS) analyses, for one of the shells with anomalously high measured content of uranium (~ 19 ppm).

4.4. Radiocarbon AMS

The preparation of the samples for radiocarbon dating was done at the National Laboratory for ^{14}C Dating, Norwegian University of Science and Technology, and AMS-measurements were carried out at the accelerator at Uppsala University, Sweden. The piece of wood (probably larch) was treated with diluted NaOH (5%) and diluted HCl (5%) to remove humic acids and carbonates, respectively. The shell (truncate softshelled clam) was etched with diluted HCl to remove the outermost part which may have been contaminated (22% removed; S. Gulliksen pers.comm. 2010). The inorganic fraction of the whale rib bone (possibly bowhead whale; Miller et al., 1989) and the bird jaw (Brünnich's guillemot) was removed by treatment with diluted HCl (25%) under vacuum and the remainder was treated with cold NaOH (5%) to remove humic acids. The collagen was then extracted with warm distilled water (pH = 3) and dried.

The one finite result has been corrected for a reservoir effect of 440 years (Mangerud et al., 2006) and calibrated according to Fairbanks et al. (2005).

5. Results

5.1. Optically stimulated luminescence

Total dose rates are between 0.60 and 1.40 Gy/ka (Table 3). Equivalent doses of the stratigraphic samples range from 29 to

156 Gy, with a corresponding age range of 36–239 ka (minimum ages 30–237 ka; Table 3). A modern analogue from the present day beach gives a low dose of 0.24 Gy. The ages largely follow stratigraphic order and group within each high sea-level event (Fig. 2, Table 3). The equivalent dose distributions are fairly wide (Fig. 8) and the average overdispersion is 15% (range 9–30%; Table 3); this is the same as the overdispersion for the dose recovery measurements (15%, see also Fig. 5). Eight of the nineteen samples are significantly positively skewed (i.e. skewness $> 2 \times$ standard error of skewness; Table 3), but for all but one sample the minimum age (Galbraith et al., 1999) overlaps with the mean age within errors. Possible causes for overdispersion and the skewed distributions are examined in the Discussion below.

From the (OSL) gamma spectrometry data, there does not appear to be any significant disequilibrium in the U-series, at least down to ^{226}Ra , except for a few samples (Fig. 9A). A plot of ^{226}Ra against ^{232}Th reveals a weak negative correlation (Fig. 9B), and HCl-dissolution of a few sediment samples shows that the $^{226}\text{Ra}/^{232}\text{Th}$ ratio seems to be strongly correlated to carbonate content.

5.2. Electron spin resonance

Analytical data and the results of ESR dating are listed in Table 4. In most cases ESR ages were determined on up to three different shell specimens taken from the same sampling point (e.g., in unit 15). The ESR analysis was performed, as a rule, on whole well-preserved aragonite shells belonging to three different boreal–arctic marine mollusc species. Due to very high uranium content in most of the shells and a correspondingly large uncertainty in the internal dose rate, their ages were calculated in two ways: (1) assuming early uptake of uranium (i.e. soon after burial) to 0.8 ppm, a typical average of uranium content (U_{in}) in the shells (Molodkov, unpublished data on more than 300 Pleistocene mollusc shells), followed very recently (late Holocene) by a rapid uptake to the measured value of U_{in} , which has practically not contributed to the growth of the time-averaged $U_{\text{in}} - \text{av}$ and, therefore, to the age calculated for $U_{\text{in}} = 0.8$ ppm; and (2) early U-uptake up to the measured value of U_{in} (Table 4). The ESR ages obtained are thus maximum and minimum values of the most probable ages. Single ages were calculated only for the two dated shells with typical U contents (about 0.8 ppm; RLQG 371-039 and 375-039, units 9 and 15, respectively).

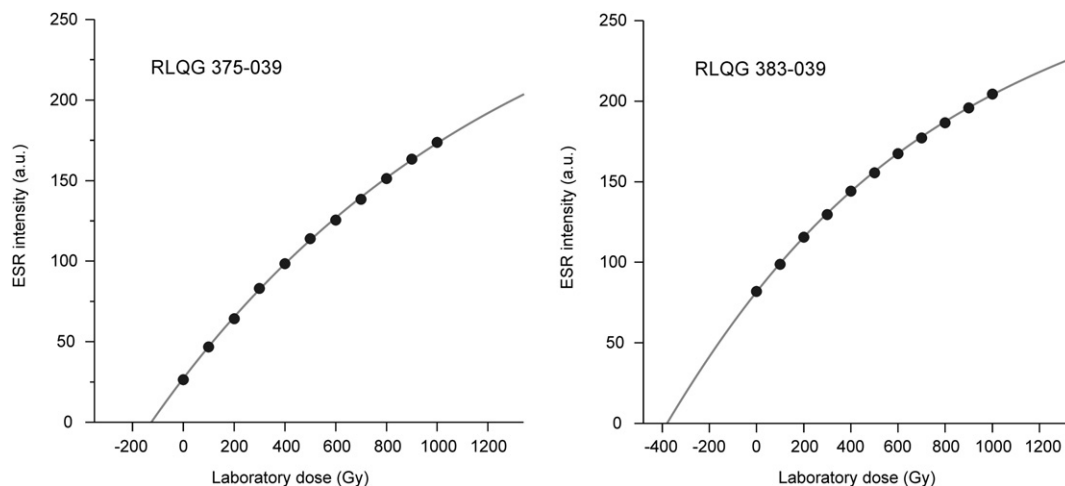


Fig. 7. Typical dose response curves of the analytical line at $g = 2.0012$ for the shell samples from the Leinstranda site. Each measurement was repeated up to 10 times for every dose and the mean taken.

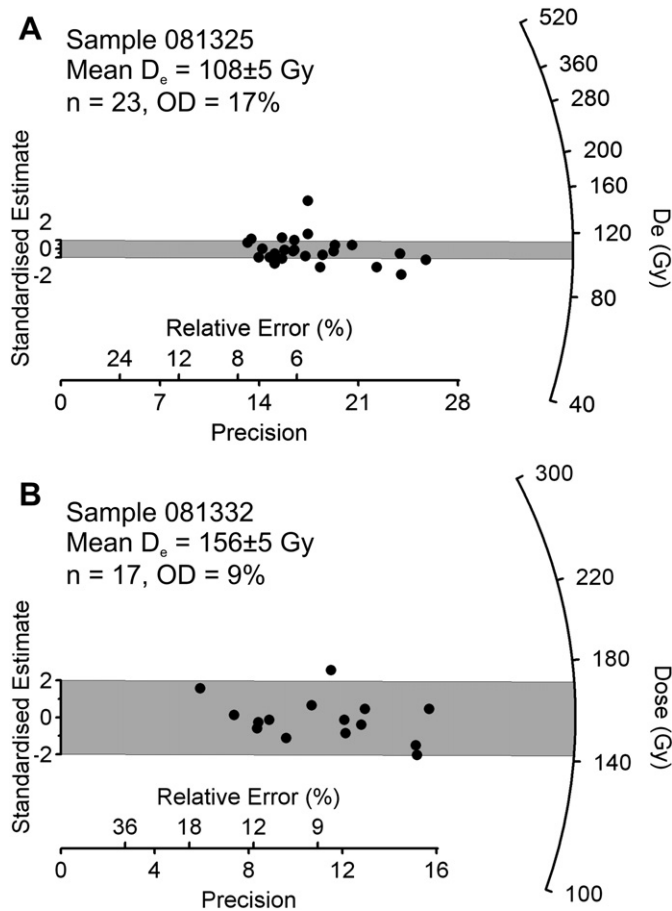


Fig. 8. Examples of dose distributions. (A). Sample 081325 (mean age 97 ± 6 ka) is a typical example with an overdispersion close to average. (B). Sample 081332 (mean age 239 ± 17 ka) is suspected of being incompletely bleached due to its significantly older age compared to the other samples from the same unit (see Table 3), but the minimum-age model did not give a significantly different age.

Thus, ESR ages of the shell samples seem to fall into three groups (from the bottom upwards): about 208 ka (MIS 7, event II), ≤ 79 ka (MIS 5a, event III) and ≤ 59 ka (MIS 4, event V). For details see Discussion section below.

5.3. Radiocarbon

Three of the four samples returned non-finite radiocarbon ages, older than $\sim 45,000$ years (Table 5). The fourth sample had a finite age (46.5 ± 0.6 cal. ka BP), although close to the measurement limit.

6. Discussion

6.1. Dosimetry

A few samples display apparent disequilibrium in the U-series. OSL-sample 081339, with a particularly low U-concentration (far left in Fig. 9A), is most noteworthy and the significantly lower age of this sample compared to the rest from the same unit (Fig. 2) may be related to the possible disequilibrium. However, the U-series usually only contributes $\sim 30\%$ of the total dose rate to quartz, and so minor uncertainties in the U dose rate contribution are not likely to be significant.

The weak negative correlation between ^{226}Ra and ^{232}Th is an unexpected pattern that may be more easily understood when the Leinstranda samples are compared with similar data from other sites in the Kongsfjorden area (Fig. 9B). It appears that many samples on Brøggerhalvøya (incl. Leinstranda) have higher ^{226}Ra contents than expected when compared to data from other sites in the area (Alexanderson & Ryen, unpublished). This may be due to the carbonate content of the sediments. Marine carbonate rocks, such as those on northern Brøggerhalvøya (Hjelle et al., 1999), are commonly relatively rich in uranium (and subsequently radium, if the U concentration is old compared to the ^{230}Th half life of ~ 80 ka) compared to thorium (cf. Cheng et al., 1998; van Calsteren and Thomas, 2006) and we believe a mixture of material from such a source and from a 'regular' (non-carbonate) source could explain the pattern we see for the Leinstranda samples.

Unusually high internal uranium content in most shells (up to ~ 19 ppm; Table 4) has led to large uncertainties in the dosimetry for the ESR-analyses and, as a result, wide ranges of possible ages. Typical uranium content in shells average about 0.8 ppm, and the internal component of radiation dose forms only a small part (usually less than 15% in average) of the total dose (Molodkov, unpublished data). Therefore, possible variation in such a relatively low U content during a shell's burial state cannot be the cause of any great deviation of the shell's age from the true one. However, if the uranium concentration in the shell is very high, the internal

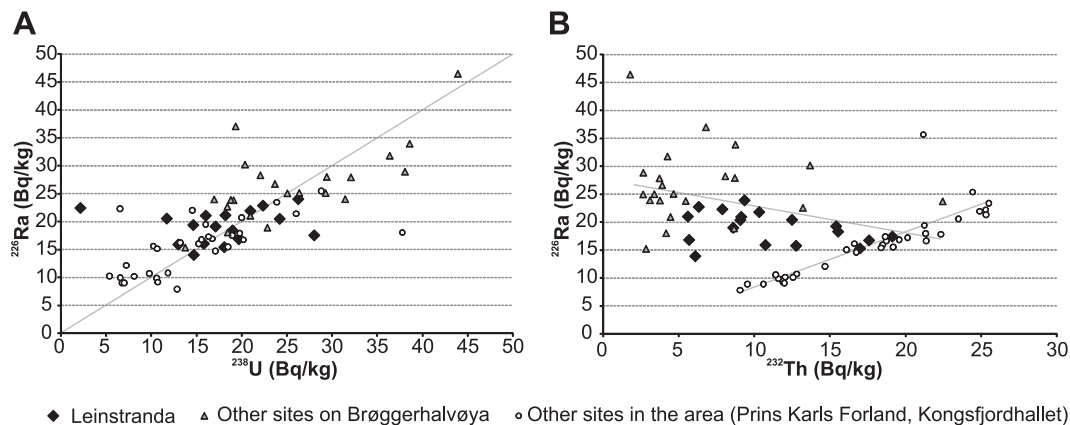


Fig. 9. Plots of radionuclide concentrations as determined by gamma spectrometry on OSL samples. The Leinstranda data are put into context with data from other sites in the area (unpublished data from Alexanderson and Ryen). (A). Plot of ^{226}Ra vs ^{238}U . Most of the samples fall at or close to a line of unity, indicating general equilibrium in the U-series. B. Plot of ^{226}Ra vs ^{232}Th . There appear to be two populations, samples from Brøggerhalvøya (incl. Leinstranda) and samples from Prins Karls Forland and Kongsfjordhallet, respectively (see Fig. 1 for location). Trendlines for these populations are shown. For further explanation and discussion, see text.

Table 4

ESR and radioactivity data for shells and enclosing sediment samples from the Leinstranda site presented in stratigraphic order. Sed. is dominant grain size of the surrounding sediment (F = fines (silt, clay), S = sand and G = gravel); P is the palaeodose; P_{in} is the internal component of palaeodose; U_{in} is the measured uranium content in the shells; U_{in-av} is the time-averaged uranium content in the shell; U, Th and K are the uranium, thorium and potassium content in the sediment as determined from laboratory gamma spectrometry.

Sample no. ^a	Unit	Mollusc species	Sed.	Depth (m)	Age ranges ^b (ka)	P (Gy)	P_{in} (Gy)	U_{in} (ppm)	U_{in-av} (ppm)	U_{sed} (ppm)	Th_{sed} (ppm)	K_{sed} (%)	Inferred age (ka) of event ^c
376-088	16	<i>Hiatella arctica</i>	S	8.0	50 – 29	68	33	6.44		1.22	5.84	1.23	V: ≤59 kaMIS 4
381-039	16	<i>Mya truncata</i>	S	9.5	111 – 46	106	73	7.40		1.29	2.45	0.77	
382-039	16	<i>Mya truncata</i>	S	9.5	127 – 41	121	93	10.97		1.29	2.45	0.77	
372-039	15	<i>Mya truncata</i>	F	10.0	64 – 36	123	60	9.00		1.88	8.45	2.25	
373-039	15	<i>Mya truncata</i>	F	10.0	58 – 35	107	49	7.40		1.88	8.45	2.25	
374-039	15	<i>Mya truncata</i>	F	10.0	65 – 36	113	56	8.00		1.88	8.45	2.25	
375-039	15	<i>Hiatella arctica</i>	F	10.0	59 ± 5	126	10	0.73		2.12	12.59	3.15	
377-088	10	<i>Mya truncata</i>	S	14.5	96 – 58	93	49	3.87		1.03	2.33	0.73	III: ≤79 kaMIS 5a
369-039	9	<i>Astarte</i> sp.	F	15.0	46 – 35	80	25	3.75		1.90	7.99	2.07	
370-039	9	<i>Astarte</i> sp.	F	15.0	52 – 38	100	32	4.40		1.90	7.99	2.07	
371-039	9	<i>Hiatella arctica</i>	F	16.0	79 ± 6	159	16	0.80		2.28	9.88	2.58	
383-039	6	<i>Hiatella arctica</i>	G	17.0	365 – 72	380	328	19.10		1.90	1.05	0.53	Reworked from MIS 9-11?
383-039-OS ^d	6	<i>Hiatella arctica</i>	G	17.0	405 ± 31	380	94		0.41				
384-039	6	<i>Hiatella arctica</i>	G	17.0	335 – 95	356	285	11.40		1.90	1.05	0.53	
379-039	6	<i>Hiatella arctica</i>	G	17.0	232 – 85	273	198	9.10		2.61	1.61	0.61	II: ~208 kareworked from MIS 7?
380-039	6	<i>Hiatella arctica</i>	G	17.0	184 – 78	208	142	7.30		2.61	1.61	0.61	

^a The laboratory code RLQG is omitted in the Table.

^b The upper age limit is for early uptake of uranium assuming a typical average of internal uranium content in the shells $U_{in} = 0.80$ ppm derived from measurements of more than 300 Pleistocene shells (Molodkov, unpublished). The lower limit is for early uptake using the measured value of U_{in} . 59 ± 5 and 79 ± 6 are ages of shells with measured U_{in} values close to typical ones and can be considered as reliable.

^c Reasons for inferring ages are discussed in the text.

^d The sample is dated by the ESR open system method (Molodkov, 1988).

dose becomes comparable with or, as in our case, even larger than the external one (Table 4).

As it was shown in an early work by Molodkov (1988), the present-day ^{230}Th activity in the shell may serve as a good indicator of time-averaged U content in the shell. Thorium is geochemically immobile. Therefore, radiogenic ^{230}Th is usually permanently fixed in the shell and its residing within the shell may meet the closed-system requirements. In view hereof, the link ^{234}U – ^{230}Th in the uranium decay chain may be considered as a low-pass filter ‘smoothing’ the ^{230}Th activity fluctuations in the shell after possible changes of U content value in it during its buried state, allowing to calculate a value of time-averaged U content in the shell from the measured ^{230}Th activity.

Thermal ionisation mass spectrometry (TIMS) measurements of the shell (RLQG 383-039) with the highest content ($U_{in} = 19.1$ ppm) have shown that the ^{230}Th activity in the shell is negligible. The time-averaged U content in this shell is calculated to be 0.4 ppm, which gives an ESR-OS age of 405 ± 31 ka (Table 4). The TIMS and ESR-OS results obtained indicate a very recent (late Holocene)

Table 5

Radiocarbon data. The calibration of sample TUA-7530 was done according to Fairbanks et al. (2005) after correcting for a reservoir age of 440 years (Mangerud et al., 2006).

Sample no.	Material	^{14}C age (years BP)		Cal. yr BP	$\delta^{13}\text{C}$
		1 σ	2 σ		
TUA-7529	Bird bone (<i>Uria lomvia</i>)	>54220	>48865	46515 ± 569	–17.8
TUA-7530	Shell (<i>Mya truncata</i>)	42045 ± 615			2.4
TUA-7531	Wood (prob. <i>Larix</i>)	>45850	>42865		–22.5
TUA-7532	Whale rib bone ^a	>49975	>46915		–16.7

^a Possibly *Balaena mysticetus* (according to find of bones at the same site/level by Miller et al., 1989).

uptake of uranium in this shell. The result allows us to consider, as very likely, the possibility of recent U uptake resulting in older ages also for other shells with high U content at this site; and thus that an age model assuming late (or recent) uranium uptake should be preferred (cf. Molodkov, 1988). This leads us to presume that the maximum ages (i.e. recent U uptake) of also most other shells at the site are to be preferred to the minimum ages.

It is most likely that the shells with the high U content took up the uranium from U-rich water that percolated through the sediments. The U content in the water need not be very high since shells are good at scavenging U. At least three potential sources of recent uranium have been identified: bedrock, sea-bird colonies and coal burning, and at least three transport agents (groundwater, surface water, precipitation). We find it unlikely that the uranium is derived by deep groundwater that has picked up uranium from the bedrock since the bedrock is not known to be particularly rich in uranium and because the thick permafrost prevents deep groundwater flow except in localised areas (e.g. Haldorsen et al., 2010). On the other hand, all samples were taken in the active layer of a coastal sediment cliff and have therefore been exposed to precipitation, surface water flow in gullies and seepage of shallow groundwater from within the active layer since the cliff retreated to near its current position. Dowdall et al. (2005) also interpreted the source of enrichment of for example ^{238}U in organic material on Brøggerhalvøya to be due to lateral flow of melt water or stream/soil water. Sea-bird colonies have been shown to give rise to elevated uranium concentrations in deposits below the nesting grounds (Dowdall et al., 2003), but there are not any large colonies within the catchment of the Leinstranda site.

We find coal mining and coal burning in the nearby former coal-mining settlement of Ny Ålesund to be the most likely source for the uranium enrichment. Radiological studies indicate elevated radioactivity in the vicinity of the mines (Dowdall et al., 2004), and local and recent contamination by other compounds related to coal burning have been shown in lake sediments on Svalbard (Rose et al.,

2004). Coal waste has been shown to contain 39–62 Bq/kg ^{238}U , 54–69 Bq/kg ^{226}Ra , 39–61 Bq/kg ^{232}Th and 499–860 Bq/kg ^{40}K (Dowdall et al., 2004) and significant enrichment of the radioisotopes occurs when the coal is combusted to ash (Baxter, 1993). Particles may have been transported directly or indirectly to our site by wind and rain/snow, and trace elements present on the surface of ash particles are readily leached and could in turn lead to soil and water contamination around the source (Carlson and Adriano, 1993; Praharaj et al., 2002; Baba and Usman, 2006).

It is in this context interesting to note that the average internal uranium contents of the shells are roughly correlated with the grain size of the surrounding sediment (gravel ~ 12 ppm, sand ~ 7 ppm and silt/clay ~ 5 ppm; Table 4). Given that the two samples with 'normal' uranium content (RLQG 371-039, 375-039) were both taken from the base of fine-grained sediment units with low permeability (Table 4, Fig. 2), it is tempting to see the amount of contamination related to sediment grain size as a reflection of permeability (i.e. amount of water the shells are exposed to). Consequently, we assume that samples 371-039 and 375-039 (lowest U_{in}) were the best protected from (U-rich) water percolation and thus from U contamination, while samples 382-039, 383-039 and 384-039 (highest U_{in}) in the coarsest units were most exposed to it. For the low- U_{in} shells uranium uptake in the very beginning of fossilisation can be assumed, as was proposed by some U-series investigators (see, e.g., Broecker, 1963; Blanchard et al., 1967), and their ages can be regarded as methodologically reliable.

The uranium enrichment is not considered to have a significant impact on the OSL ages since quartz does not absorb U and the very recent enrichment of the groundwater has not been able to cause noticeable deviation of the secular external dose rate from the measured one.

The amount of water, or ice, in the sediment is also important in the calculation of the final dose rate, as it absorbs some of the radiation that would otherwise have reached the measured quartz grains or shells. We assumed water contents close to saturation during the time since deposition. Since saturation (porosity) values set an upper limit to possible water contents (<3 percentage point change from stated values, Table 3) we believe that the samples are unlikely to have much lower dose rates (i.e. to be much older). Mean water content could have been lower, however, and dose rates correspondingly higher, making the ages younger. To that end, a lower limit is set by water content at sampling, and in the extreme case by completely dry sediments, but the latter must be

considered unlikely. Using the water content at sampling as mean water content since deposition would make OSL ages about $\sim 15\%$ younger, but still within one standard deviation of the ages presented in Table 3. We do not believe that the water content has changed that much and a smaller water content change would not make much difference to the OSL and ESR ages.

6.2. OSL – incomplete bleaching and other factors affecting the dose or age

With long polar nights and proximity to glaciers, sediments at Leinstranda run a risk of suffering from incomplete bleaching due to insufficient exposure to sunlight at the time of deposition (Bateman and Murton, 2006; Bateman, 2008; Fuchs and Owen, 2008). Luminescence analyses of modern sediments from depositional environments similar to those sampled at Leinstranda indicate that shallow marine and littoral sediments generally are bleached, with doses of less than 1 Gy, at most 5 Gy (Alexanderson et al., unpublished data). Similarly, for late Weichselian and Holocene beaches there is no significant overestimation of OSL ages compared to calibrated radiocarbon ages of shells from the same site and stratigraphic level (Svensson, 2009; Ryen et al., unpublished data). The consistent OSL ages within sedimentary units (Fig. 2) also suggest that bleaching at Leinstranda was sufficient. If incomplete bleaching had occurred, all grains (sediment beds) are unlikely to have been bleached to the same degree and thus would not be expected to give similar ages. Although skewness and overdispersion is significant for the D_e distributions of some samples (Table 3), none of these 'bad' samples differ significantly in age from 'good' ones ($OD < 15\%$, skewness $< 2 \times$ standard error of skewness) from the same unit. Nor are the minimum ages significantly different from the mean ages, which would be expected if there was a large population of poorly bleached grains (cf. Olley et al., 2004). Also, similar values of overdispersion have been documented elsewhere for multi-grain aliquots of well-bleached sediments (e.g. Jacobs et al., 2003b; Galbraith et al., 2005; Lian and Roberts, 2006). This suggests that the spread in doses is likely not related to incomplete bleaching but rather to material characteristics or other factors (e.g. beta dose heterogeneity, feldspar contamination). If the scatter is not related to incomplete bleaching, the value of the minimum-age model is reduced (Galbraith et al., 1999; Bailey and Arnold, 2006) and therefore we use the mean ages as the final ones.

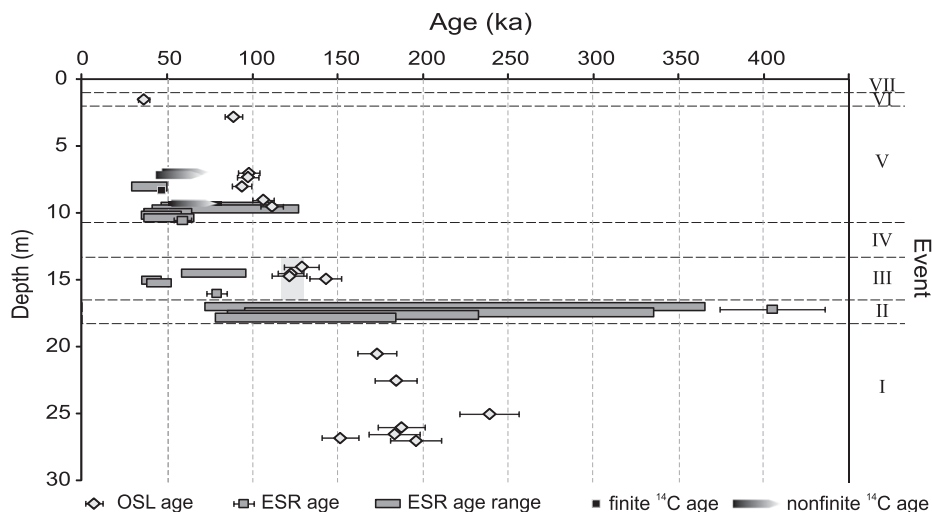


Fig. 10. A plot of our OSL, ESR and ^{14}C ages against depth and interpreted high relative sea-level events. The grey square denotes the Eemian interglacial (MIS 5e). The OSL chronology provides largely stratigraphically consistent ages, while the ESR ages are younger in the upper part and overlap or are older in the lower part.

Available data from the area thus suggest that any effect of incomplete bleaching is likely to be small, in the order of a few hundred (≤ 1 Gy) to a few thousand years (2–5 Gy), well within the error limits of the Leinstranda samples. This is in accordance with estimates of the effects of incomplete bleaching from late Quaternary glaciomarine/glaciolacustrine settings in Greenland (Hansen et al., 1999) and Scandinavia (e.g. Kortekaas et al., 2007), although larger amounts have been documented (e.g. Rhodes and Pownall, 1994; Alexanderson and Murray, in press). It should, however, be noted that with large single aliquots it is difficult to resolve partial bleaching (Olley et al., 1999; Duller, 2008), and so the possibility that some samples are nonetheless incompletely bleached must be left open.

Other factors that may influence the accuracy of OSL dose estimates and ages include thermal transfer and feldspar contamination (e.g. Rhodes, 2000; Jacobs et al., 2003a). Preheat plateau tests (Fig. 3) and low recuperation values suggest that thermal transfer is insignificant for the chosen temperature settings and should not contribute to any dose (age) overestimate. Likewise, feldspar contamination appears to be insignificant.

6.3. Method comparison

The methods and the resulting chronologies have their strengths and weaknesses and we will discuss these, focussing on the OSL- and ESR-chronologies, and explaining differences and similarities of the results where possible. It is important to note that OSL and ESR are not truly independent methods although they make use of different ‘time-recording’ mechanisms. For example, the dosimetry is much the same and anything that affects the dosimetry for one of the methods, will also affect the other method and in the same direction. Thus, if we for example lower the ESR dose rates to make the ESR ages older – and more comparable to the OSL ages – we also need to lower the OSL dose rates and the OSL ages will be even older.

The OSL chronology provides broadly stratigraphically consistent ages (two exceptions in Event I can be explained, see below), both within and between sedimentary units, and internal methodological tests show that the samples behave satisfactorily (Fig. 2). Likewise, the ESR chronology from Leinstranda, if based on the assumption of very recent U uptake in shells, also provides largely stratigraphically consistent ages (Fig. 2), with the exception of a few age inversions that have to be explained (see below). However, the results from the different dating techniques do not agree completely. The well constrained ESR ages are in almost all cases younger than corresponding OSL ages, or, for the large ESR age ranges, the mean is lower than that of the OSL ages (Fig. 10). For the two events where we have both ESR and OSL ages (III, V), there appears to be a systematic difference of roughly 50 ka between the results from the two methods.

A probable cause for OSL age overestimation is incomplete bleaching, but all available data suggest that the effect is limited to at most a few thousand years. It is also unlikely to affect the ages from several samples from two separate events with the same amount of overestimation. Uncertainties in dosimetry, especially water content, could make the ages somewhat younger, but would affect the ESR ages as well, as mentioned above (e.g. Fig. 10). Thus, it seems difficult to explain the disagreement by changing the input parameters to the OSL ages within reasonable bounds.

To make the ESR ages older, higher palaeodoses and/or lower dose rates are needed. Analytically, there seems to be little potential for such changes: palaeodoses have been determined very precisely, frequently on several different shells; and the lowest possible dose rates have been applied by the assumption that U uptake in the shells occurred very recently. Theoretically, low stability of the ESR

signal may result in underestimation of the true ages, especially for older samples. However, stability of the ESR signal is favoured at Svalbard by a relatively low burial temperature: even at the present interglacial air temperature of ca -6 °C (average 1961–90; Norwegian Meteorological Institute), the mean lifetime of the signal at $g = 2.0012$ in the typical marine shells from Arctic region is sufficiently long – about 10^7 years (Molodkov, 1989) – to prevent any underestimation of the shell ESR ages even for those from the lowest stratigraphic level. Also, the reliability of the over-modulation measurement technique of the $g = 2.0012$ analytical signal (Molodkov, 1988, 1993) is supported by results from the Intercomparison Project on ESR-Dating (Barabas et al., 1993; lab. no 6) and by results of parallel dating between ESR closed system, ESR open system, IRSL and U–Th (Molodkov and Bolikhovskaya, 2010; Molodkov, unpublished data).

Three of the four new radiocarbon ages are non-finite, older than ~ 45 – 50 ^{14}C ka BP, and thus do not contradict either OSL or ESR results. The one finite age, 46.5 ± 0.6 cal. ka BP from a mollusc shell (Table 5), is analytically finite, but in the context of being surrounded by non-finite ages it should be regarded as a minimum age (S. Gulliksen, pers.comm. 2010). A too young age for the shell could be due to contamination from younger carbon (cf. Sulerzhitsky, 1998; Houmark-Nielsen and Funder, 1999).

Units 9–11 (event III) are interpreted to be deposited during interglacial conditions, based on their microfossil content (Miller et al., 1989) and macrobenthic fauna, particularly the occurrence of *Astarte borealis* (S. Funder, pers.comm., unpublished data). The ages from units 9–11 that best correspond to a known interglacial, in this case the last interglacial (MIS 5e), are the OSL ages, which average 129 ± 10 ka, while the other ages are significantly younger (Fig. 2). By inference, it would be likely to assume that OSL is working well also for the other events; but this is discussed in more detail for each event below.

7. Chronology of high relative sea-level events

7.1. High sea-level events I and II

Event I represents regression from an initially high sea-level right after a deglaciation and is followed by (likely) raised relative sea-level as glaciers approached the site anew during event II (Alexanderson et al., 2011). Of the seven OSL ages from units 2 and 3 (event I; Fig. 2), there are two outliers, one younger and one older than the remaining five which are consistent within errors. These outliers could possibly be explained by odd dosimetry (see above)

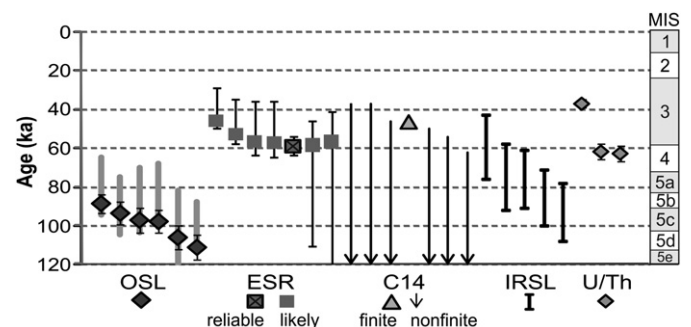


Fig. 11. Absolute ages from units 15–17 (high sea level event V) at Leinstranda, cf. Fig. 2, illustrating how ages of one event may differ between methods. The grey lines at the OSL ages represent the theoretical age ranges calculated using different water contents (see text for explanation). See text also for discussion on methodologically likely ESR ages. Data are from this study and from Miller et al. (1989) and Forman (1999).

and incomplete bleaching, respectively. The mean OSL age of event I is 185 ± 8 ka.

The ESR ages from the overlying unit 6 (event II; Fig. 2), have a wide range of maximum ages from 184 to 405 ka. As it was reported above, supplementary isotope analyses and ESR-OS dating of sample RLQG 383-039 suggest that U-uptake in the shell occurred very recently, most likely within the last hundred years. Therefore, we assume that the rest of the shells taken from the gravelly unit were also recently enriched with uranium and consequently their ages are rather close to the maximum estimates. Nevertheless, there is an apparent inversion of the ages obtained on two pairs of different shells. The older ones were taken from sand pockets within a pebbly–bouldery deposit, and it could be that the sediment dose rate as measured from the sample is not entirely representative. Or, if the ages are taken at face value, the older shells were reworked from older deposits of middle Pleistocene age. In that case an average age between 236 and 208 ka can be calculated for the younger pair of shells with U content of 0.4 and 0.8 ppm, respectively.

Considering the uncertainties associated with both ages, an ESR-age of ~ 208 ka for unit 6 is not incompatible with the ~ 185 ka OSL ages from the underlying units. The two events I and II could be close in time, or the shells in unit 6 could be redeposited from older strata. The latter could also explain the difference in ages between the ESR samples from the same unit. Based on amino acid chronology of shells, Miller et al. (1989) inferred an age of at least 160 ka for their zone D (our event I); this does not contradict either chronology. From the available data we therefore conclude that our events I and II correlate to regional high sea-level event(s) during MIS 6 or late MIS 7, ~ 185 ka.

7.2. High sea-level events III and IV

During event III a relative high sea-level right after the deglaciation of a major ice sheet was gradually lowered due to isostatic rebound (Fig. 2; Alexanderson et al., 2011). From the microfossil content of sediments, Miller et al. (1989) concluded that marine conditions during our event III (part of their zone C) were more favourable than during the Holocene. This is in line with evidence from the macrobenthic fauna (S. Funder, pers.comm.). We, like Miller et al. (1989), therefore correlate this event with MIS 5e, when inflow of Atlantic water was large and sustained (cf. Hald et al., 2001), and infer an interglacial situation. The OSL (and IRSL) ages, which for event III average 129 ± 10 ka (IRSL 140 ± 20 ka; Forman, 1999), are the ones that best agree with a last interglacial age. The ESR ages are considerably younger ($\leq 79 \pm 6$ ka), as well as also the single U/Th (on *Hiattella arctica*; Miller et al., 1989) and TL ages (Troitsky et al., 1979) (Fig. 2), and rather correlate with MIS 5a.

Event IV could not be dated since no datable material was found.

7.3. High sea-level event V

Similar to event III, event V represents post-glacial regression (Alexanderson et al., 2011). The microfauna (in zone B deposits; Miller et al., 1989) suggest that nearshore conditions were similar to those during the Holocene. This implies favourable conditions likely due to Atlantic water inflow, but taken at face value, age ranges from the different methods each overlap with one or more of those inflow events (Hald et al., 2001). Our high sea-level event V may be correlated to inflow taking place during MIS 5c (OSL 99 ± 8 ka), MIS 5a (IRSL 80 ± 10 ka) or late MIS 4 to early MIS 3 (ESR 59 ± 5 ka to ~ 50 ka) (Fig. 10). Perhaps more relevant is that the event needs to have been preceded by a major glaciation to give rise to the significant isostatic loading required for the (presently) raised marine deposits. Such glaciations have been documented to occur in the Barents Sea area both in MIS 5 (post MIS 5e) and in MIS 4/3 (Mangerud et al., 1998; Svendsen et al., 2004).

The ESR age ranges partly overlap the OSL ages (127–41 and 111–46 ka), partly they are younger (≤ 59 ka). A higher time-averaged U-content and thus true ages towards the younger end of the age range would correspond with the one finite ^{14}C age (46.5 cal. ka BP, Table 5) from the same part of unit 16.

All available ages for units 15–17 are shown in Fig. 11. We interpret the event to have lasted at most $\sim 10,000$ years (if compared to the last deglaciation) and the ages can therefore be taken as dating one event within the resolution of most of the methods at these age ranges. The radiocarbon and U/Th ages, which both are considered minimum ages (see above and Miller et al., 1989), suggest that event V is older than ~ 45 –60 ka. The OSL ages indicate a MIS 5 age and their accuracy is supported by the agreement between the biostratigraphically inferred interglacial and the OSL ages of event III. This would indicate that MIS 5c, or 5a, are more likely candidates than stages 4/3, which the ESR ages suggest. Based on the above, we interpret event V to be an early Weichselian interstadial, but an early middle Weichselian age cannot be ruled out.

7.4. High sea-level events VI and VII

Event VI is represented only by a thin gravelly-sandy bed between hiatuses (Fig. 2) and only a single OSL age (36 ± 3 ka) is available. However, deposits with similar OSL ages have been identified also at other sites in the area (H.T. Ryen, unpublished data) and lend support to a middle Weichselian age.

Geomorphologically pronounced beach ridges make up the deposits of event VII. The event has not been dated by us, but Miller et al. (1989) present single radiocarbon and U/Th ages from a nearby site that give an early Holocene age. The elevation of the beaches is also in line with highest deglacial marine limits at other sites in the area (Forman and Miller, 1984; Forman et al., 1987; Forman, 1989) and a last deglaciation age is concluded.

Table 6
Summary of ages (in ka; cal. ka for ^{14}C -ages) and concluded timing of events.

Event	OSL	ESR	^{14}C	U/Th ^b	IRSL ^c	TL ^d	Amino ^b	Alt. 1	Alt. 2
VII			10.7 ± 0.3^a	8 ± 2				Early Holocene, ~ 11 ka	Early Holocene, ~ 11 ka
VI	36 ± 3							Middle Weichselian, 40–30 ka	Middle Weichselian, 40–30 ka
V	99 ± 8	≤ 59	≥ 46	≥ 60	80 ± 10		70 ± 10	Early Weichselian, 110–90 ka	Middle Weichselian, 60–45 ka
IV									
III	129 ± 10	≤ 79		≥ 65	140 ± 20	53	125 ± 10	Eemian, 140–120 ka	Early Weichselian, 80–65 ka
II								Saalian, 200–170 ka	
I	185 ± 8						> 160		

^a Miller et al. (1989). Calibrated by us using Fairbanks et al. (2005) after reservoir correction of 440 yr (Mangerud et al., 2006).

^b Inferred ages according to Miller et al. (1989).

^c Inferred ages according to Forman (1999).

^d Troitsky et al. (1979).

8. Conclusions

Raised glaciomarine, shallow marine and littoral deposits at Leinstranda, NW Svalbard, have been dated by optically stimulated luminescence (OSL), electron spin resonance (ESR) and radiocarbon (AMS-¹⁴C). OSL dating was done on sand-sized quartz from raised shallow marine and littoral sediments. The quartz was bright with a clear signal dominated by the fast component. ESR dating was performed on *M. truncata*, *H. arctica* and *Astarte* sp. mollusc shells from glaciomarine and shallow marine sediments. Unusually high uranium content in some shells (≤ 19 ppm) led to large uncertainties in the final ages for those samples. The high uranium content may be due to significant recent uranium enrichment of the shells, possibly related to contamination from coal burning in a nearby mining settlement.

Ages from the site range from the Saalian s.l. (\geq MIS 6) to the early Holocene (MIS 1). Both OSL and ESR provide broadly stratigraphic consistent ages, with OSL ages generally being more precise than ESR. The absolute ages of events differ between the two methods – there is a systematic offset between OSL- and ESR-ages – and two alternative chronologies for the seven high relative sea-level events identified in the Leinstranda section (Fig. 2; cf. Alexanderson et al., 2011), are presented, see Table 6. The cause of this age difference between methods remains to be determined. Based on currently available data, including a better agreement of OSL ages with other evidence, we base our chronology of sea-level change and glaciations on the OSL ages, but we cannot rule out the ESR ages.

Our results contribute to the knowledge of the timing of glacial and non-glacial events on Svalbard during the middle and late Quaternary, and thereby also to our understanding of glacial dynamics and environmental change in a highly sensitive part of the world – the Arctic.

Acknowledgements

We hereby gratefully acknowledge the excellent field assistance provided by Mikael Lindqvist and Gustaf Peterson (Stockholm University) and the logistic support from the Norwegian Polar Institute, especially Wojciech Moskal, in Ny Ålesund. Thanks also to Heidi T. Ryen (Norwegian University of Life Sciences) and Svend Funder (Geological Museum, Copenhagen) who generously shared unpublished data, and Sébastien Huot (Université du Québec à Montréal) who shared his excel-macros for the minimum-age model and for calculating overdispersion. Help with species identification of fossils was provided by Svend Funder, Geological Museum, Copenhagen (mollusc shells), Anne Karin Hufthammer, Bergen Museum (bird bones) and Helge I. Høeg, Larvik (wood). The assistance of Erdem Bekaroğlu (Ankara University) with TIMS analysis and Evelin Verš (Institute of Geology, Tallinn University of Technology) with ICP MS analysis are gratefully acknowledged. We also wish to thank Tatyana Balakhnichova and Marina Osipova (RLQG) for their contribution to the ESR work reported here. Two anonymous reviewers gave constructive criticism that improved the paper. This study was part of the Research Council of Norway-funded project SciencePub, which is a contribution to the International Polar Year 2007–2008. The Estonian Science Foundation (grant no. 8425) is also acknowledged for partial support of this work.

Editorial handling by: R. Roberts

References

- Adamiec, G., Aitken, M., 1998. Dose-rate conversion factors: update. *Ancient TL* 16 (2), 37–50.
- Aitken, M.J., 1998. *An Introduction to Optical Dating*. Oxford University Press, Oxford.

- Alexanderson, H., Murray, A.S. Problems and potential of OSL dating Weichselian and Holocene sediments in Sweden. *Quaternary Science Reviews*, in press, doi: 10.1016/j.quascirev.2009.09.020.
- Alexanderson, H., Landvik, J.Y., Ryen, H.T., 2011. Chronology and styles of glaciation in an inter-fjord setting, northwestern Svalbard. *Boreas* 40 (1), 175–197.
- Bøtter-Jensen, L., Bulur, E., Duller, G.A.T., Murray, A.S., 2000. Advances in luminescence instrument systems. *Radiation Measurements* 32 (5–6), 523–528.
- Baba, A., Usmen, M., 2006. Effects of fly ash from coal-burning electrical utilities on ecosystem and utilization of fly ash. In: Baba, A., Howard, K., Gunduz, O. (Eds.), *Groundwater and Ecosystems*. Springer, Netherlands, pp. 15–31.
- Bailey, R.M., Arnold, L.J., 2006. Statistical modelling of single grain quartz De distributions and an assessment of procedures for estimating burial dose. *Quaternary Science Reviews* 25 (19–20), 2475–2502.
- Bailey, R.M., Smith, B.W., Rhodes, E.J., 1997. Partial bleaching and the decay form characteristics of quartz OSL. *Radiation Measurements* 27 (2), 123–136.
- Barabas, M., Walther, R., Wieser, A., Radtke, U., Grün, R., 1993. Second interlaboratory-comparison project on ESR dating. *Applied Radiation and Isotopes* 44 (1–2), 119–129.
- Bateman, M.D., 2008. Luminescence dating of periglacial sediments and structures. *Boreas* 37 (4), 574–588.
- Bateman, M.D., Murton, J.B., 2006. The chronostratigraphy of Late Pleistocene glacial and periglacial aeolian activity in the Tuktoyaktuk Coastlands, NWT, Canada. *Quaternary Science Reviews* 25 (19–20), 2552–2568.
- Baxter, M.S., 1993. Environmental radioactivity: a perspective on industrial contributions. *IAEA Bulletin* 35, 33–38.
- Berger, G.W., 2006. Trans-arctic-ocean tests of fine-silt luminescence sediment dating provide a basis for an additional geochronometer for this region. *Quaternary Science Reviews* 25 (19–20), 2529–2551.
- Blanchard, R.L., Cheng, M.H., Portratz, H.A., 1967. Uranium and thorium series equilibria in recent and fossil marine molluscan shells. *Journal of Geological Research* 72, 4745–4757.
- Broecker, W.S., 1963. A preliminary evaluation of uranium series in equilibrium as a tool for absolute age measurements on marine carbonates. *Journal of Geophysical Research-Earth Surface* 68, 2817–2834.
- Carlson, C.L., Adriano, D.C., 1993. Environmental impacts of coal combustion residues. *Journal of Environmental Quality* 22 (2), 227–247.
- Cheng, H., Edwards, R.L., Murrell, M.T., Benjamin, T.M., 1998. Uranium-thorium-protactinium dating systematics. *Geochimica et Cosmochimica Acta* 62 (21–22), 3437–3452.
- Choi, J.H., Duller, G.A.T., Wintle, A.G., 2006. Analysis of quartz LM-OSL curves. *Ancient TL* 24 (1), 9–20.
- Cunningham, A.C., Wallinga, J., 2010. Selection of integration time intervals for quartz OSL decay curves. *Quaternary Geochronology* 5 (6), 657–666.
- Dowdall, M., Gerland, S., Lind, B., 2003. Gamma-emitting natural and anthropogenic radionuclides in the terrestrial environment of Kongsfjord, Svalbard. *The Science of the Total Environment* 305 (1–3), 229–240.
- Dowdall, M., Vicat, K., Frearson, I., Gerland, S., Lind, B., Shaw, G., 2004. Assessment of the radiological impacts of historical coal mining operations on the environment of Ny-Ålesund, Svalbard. *Journal of Environmental Radioactivity* 71 (2), 101–114.
- Dowdall, M., Gwynn, J.P., Moran, C., Davids, C., O’Dea, J., Lind, B., 2005. Organic soil as a radionuclide sink in a High Arctic environment. *Journal of Radioanalytical and Nuclear Chemistry* 266 (2), 217–223.
- Duller, G.A.T., 2003. Distinguishing quartz and feldspar in single grain luminescence measurements. *Radiation Measurements* 37 (2), 161–165.
- Duller, G.A.T., 2004. Luminescence dating of Quaternary sediments: recent advances. *Journal of Quaternary Science* 19, 183–192.
- Duller, G.A.T., 2008. Single-grain optical dating of Quaternary sediments: why aliquot size matters in luminescence dating. *Boreas* 37 (4), 589–612.
- Fairbanks, R.G., Mortlock, R.A., Chiu, T.-C., Cao, L., Kaplan, A., Guilderson, T.P., Fairbanks, T.W., Bloom, A.L., Grootes, P.M., Nadeau, M.-J., 2005. Radiocarbon calibration curve spanning 0 to 50,000 years BP based on paired ²³⁰Th/²³⁴U/²³⁸U and ¹⁴C dates on pristine corals. *Quaternary Science Reviews* 24 (16–17), 1781–1796.
- Forman, S.L., 1989. Late Weichselian glaciation and deglaciation of Forlandsundet area, western Spitsbergen, Svalbard. *Boreas* 18, 51–60.
- Forman, S.L., 1999. Infrared and red stimulated luminescence dating of Late Quaternary near-shore sediments from Spitsbergen, Svalbard. *Arctic, Antarctic, and Alpine Research* 31 (1), 34–49.
- Forman, S.L., Miller, G.H., 1984. Time-dependent soil morphologies and pedogenic processes on raised beaches, Brøggerhalvøya, Spitsbergen, Svalbard archipelago. *Arctic and Alpine Research* 16 (4), 381–394.
- Forman, S.L., Mann, D.H., Miller, G.H., 1987. Late Weichselian and Holocene relative sea-level history of Brøggerhalvøya, Spitsbergen. *Quaternary Research* 27 (1), 41–50.
- Forman, S.L., Lubinski, D.J., Ingólfsson, Ó., Zeeberg, J.J., Snyder, J.A., Siegert, M.J., Matishov, G.G., 2004. A review of postglacial emergence on Svalbard, Franz Josef land and Novaya Zemlya, northern Eurasia. *Quaternary Science Reviews* 23 (11–13), 1391–1434.
- Fuchs, M., Owen, L.A., 2008. Luminescence dating of glacial and associated sediments: review, recommendations and future directions. *Boreas* 37 (4), 636–659.
- Galbraith, R.F., Roberts, R.G., Laslett, G.M., Yoshida, H., Olley, J.M., 1999. Optical dating of single and multiple grains of quartz from Jimmum rock shelter, northern Australia. Part I: experimental design and statistical models. *Archaeometry* 41 (2), 339–364.

- Galbraith, R.F., Roberts, R.G., Yoshida, H., 2005. Error variation in OSL palaeodose estimates from single aliquots of quartz: a factorial experiment. *Radiation Measurements* 39 (3), 289–307.
- Grün, R., 1989. Electron spin resonance (ESR) dating. *Quaternary International* 1, 65–109.
- Grün, R., 1991. Potential and problems of ESR dating. *International Journal of radiation applications and Instrumentation. Part D. Nuclear Tracks and Radiation Measurements* 18 (1–2), 143–153.
- Hald, M., Dokken, T., Mikalsen, G., 2001. Abrupt climatic change during the last interglacial-glacial cycle in the polar North Atlantic. *Marine Geology* 176 (1–4), 121–137.
- Haldorsen, S., Heim, M., Dale, B., Landvik, J.Y., van der Ploeg, M., Leijnse, A., Salvigsen, O., Hagen, J.O., Banks, D., 2010. Sensitivity to long-term climate change of subpermafrost groundwater systems in Svalbard. *Quaternary Research* 73 (2), 393–402.
- Hansen, L., Funder, S., Murray, A.S., Mejdahl, V., 1999. Luminescence dating of the last Weichselian glacier advance in East Greenland. *Quaternary Geochronology (Quaternary Science Reviews)* 18, 179–190.
- Hjelle, A., Piepjohn, K., Saalmann, K., Ohta, Y., Salvigsen, O., Thiedig, F., Dallmann, W.K., 1999. Geological Map of Svalbard 1:100,000, Sheet A7G Kongsfjorden. Norsk Polarinstitut.
- Houmark-Nielsen, M., Funder, S., 1999. Pleistocene stratigraphy of Kongsfjordhallet, Spitsbergen, Svalbard. *Polar Research* 18 (1), 39–49.
- Humlum, O., Instanes, A., Sollid, J.L., 2003. Permafrost in Svalbard: a review of research history, climatic background and engineering challenges. *Polar Research* 22 (2), 191–215.
- Ikeya, M., 1985. Dating methods of Pleistocene deposits and their problems: IX. Electron spin resonance. In: Rutter, N.W. (Ed.), *Dating Methods of Pleistocene Deposits and Their Problems*. Geoscience, Canada, pp. 73–87. Reprint Series.
- Ikeya, M., Ohmura, K., 1981. Dating of fossil shells with electron spin resonance. *Journal of Geology* 89, 247–251.
- Jacobs, Z., 2008. Luminescence chronologies for coastal and marine sediments. *Boreas* 37 (4), 508–535.
- Jacobs, Z., Duller, G.A.T., Wintle, A.G., 2003a. Optical dating of dune sand from Blombos Cave, South Africa: II—single grain data. *Journal of Human Evolution* 44, 613–625.
- Jacobs, Z., Wintle, A.G., Duller, G.A.T., 2003b. Optical dating of dune sand from Blombos Cave, South Africa: I—multiple grain data. *Journal of Human Evolution* 44 (5), 599–612.
- Jain, M., Choi, J.H., Thomas, P.J., 2008. The ultrafast OSL component in quartz: Origins and implications. *Radiation Measurements* 43 (2–6), 709–714.
- Jakobsson, M., Backman, J., Murray, A., Løvlie, R., 2003. Optically Stimulated Luminescence dating supports central Arctic Ocean cm-scale sedimentation rates. *Geochemical Geophysics Geosystem* 4 (2), 1016.
- Katzenberger, O., Willems, N., 1988. Interferences encountered in the determination of AD of mollusc samples. *Quaternary Science Reviews* 7 (3–4), 485–489.
- Kjær, K.H., Demidov, I.N., Larsen, E., Murray, A., Nielsen, J.K., 2003. Mezen Bay – a key area for understanding Weichselian glaciations in northern Russia. *Journal of Quaternary Science* 18 (1), 73–93.
- Kjær, K.H., Larsen, E., Funder, S., Demidov, I.N., Jensen, M., Håkansson, L., Murray, A., 2006. Eurasian ice-sheet interaction in northwestern Russia throughout the late Quaternary. *Boreas* 35 (3), 444–475.
- Kortekaas, M., Murray, A.S., Sandgren, P., Björck, S., 2007. OSL chronology for a sediment core from the southern Baltic Sea: a continuous sedimentation record since deglaciation. *Quaternary Geochronology* 2 (1–4), 95–101.
- Lian, O.B., Roberts, R.G., 2006. Dating the Quaternary: progress in luminescence dating of sediments. *Quaternary Science Reviews* 25, 2449–2468.
- Liestøl, O., 1976. Pingos, Springs, and Permafrost in Spitsbergen. *Årbok 1975*. Norsk Polarinstitut, Oslo, 19757–29.
- Möller, P., Fedorov, G., Pavlov, M., Seidenkrantz, M.-S., Sparrenbom, C., 2008. Glacial and palaeoenvironmental history of the Cape Chelyuskin area, arctic Russia. *Polar Research* 27 (2), 222–248.
- Mangerud, J., Dokken, T., Hebbeln, D., Heggen, B., Ingólfsson, Ó., Landvik, J.Y., Mejdahl, V., Svendsen, J.I., Vorren, T.O., 1998. Fluctuations of the Svalbard-Barents Sea ice sheet during the last 150,000 years. *Quaternary Science Reviews* 17, 11–42.
- Mangerud, J., Bondevik, S., Gulliksen, S., Hufthammer, A.K., Høisæter, T., 2006. Marine ¹⁴C reservoir ages for 19th century whales and molluscs from the North Atlantic. *Quaternary Science Reviews* 25 (23–24), 3228–3245.
- McLaren, S.J., Rowe, P.J., 1996. The reliability of uranium-series mollusc dates from the western mediterranean basin. *Quaternary Science Reviews* 15 (7), 709–717.
- Miller, G.H., 1982. Quaternary depositional episodes, western Spitsbergen, Norway: aminostratigraphy and glacial history. *Arctic and Alpine Research* 14 (4), 321–340.
- Miller, G.H., Sejrup, H.P., Lehman, S.J., Forman, S.L., 1989. Glacial history and marine environmental change during the last interglacial-glacial cycle, western Spitsbergen, Svalbard. *Boreas* 18, 273–296.
- Molodkov, A., 1986. Application of ESR to the dating of subfossil shells from marine deposits. *Ancient TL* 4, 49–54.
- Molodkov, A., 1988. ESR dating of Quaternary shells: recent advances. *Quaternary Science Reviews* 7, 477–484.
- Molodkov, A., 1989. The problem of long-term fading of absorbed palaeodose on ESR-dating of Quaternary mollusc shells. *Applied Radiation and Isotopes* 40, 1087–1093.
- Molodkov, A., 1993. ESR-dating of non-marine mollusc shells. *Applied Radiation and Isotopes* 43, 145–148.
- Molodkov, A., 2001. ESR dating evidence for early man at a Lower Palaeolithic cave-site in the Northern Caucasus as derived from terrestrial mollusc shells. *Quaternary Science Reviews* 20 (5–9), 1051–1055.
- Molodkov, A.N., Bolikhovskaya, N.S., 2002. Eustatic sea-level and climate changes over the last 600 ka as derived from mollusc-based ESR-chronostratigraphy and pollen evidence in Northern Eurasia. *Sedimentary Geology* 150 (1–2), 185–201.
- Molodkov, A., Bolikhovskaya, N., 2009. Climate change dynamics in Northern Eurasia over the last 200 ka: evidence from mollusc-based ESR-chronostratigraphy and vegetation successions of the loess-palaeosol records. *Quaternary International* 201 (1–2), 67–76.
- Molodkov, A., Bolikhovskaya, N., 2010. Climato-chronostratigraphic framework of Pleistocene terrestrial and marine deposits of Northern Eurasia, based on pollen, electron spin resonance, and infrared optically stimulated luminescence analyses. *Estonian Journal of Earth Sciences* 59 (1), 49–62.
- Molodkov, A., Dreimanis, A., Āboltiņš, O., Raukas, A., 1998. The ESR age of *Portlandia arctica* shells from glacial deposits of Central Latvia: an answer to a controversy on the age and genesis of their enclosing sediments. *Quaternary Science Reviews* 17, 1077–1094.
- Molodkov, A., Bolikhovskaya, N., Gaigalas, A., 2002. The last Middle Pleistocene interglacial in Lithuania: insights from ESR-dating of deposits at Valakampiai, and from stratigraphic and palaeoenvironmental data. *Geological Quarterly* 46 (4), 363–374.
- Murray, A.S., Wintle, A.G., 2000. Luminescence dating of quartz using an improved single-aliquot regenerative-dose protocol. *Radiation Measurements* 32 (1), 57–73.
- Murray, A.S., Wintle, A.G., 2003. The single aliquot regenerative dose protocol: potential for improvements in reliability. *Radiation Measurements* 37 (4–5), 377–381.
- Murray, A.S., Marten, R., Johnson, A., Martin, P., 1987. Analysis for naturally occurring radionuclides at environmental concentrations by gamma spectrometry. *Journal of Radioanalytical and Nuclear Chemistry Articles* 115, 263–288.
- Olley, J.M., Caitcheon, G.G., Roberts, R.G., 1999. The origin of dose distributions in fluvial sediments, and the prospect of dating single grains from fluvial deposits using optically stimulated luminescence. *Radiation Measurements* 30, 207–217.
- Olley, J.M., Pietsch, T., Roberts, R.G., 2004. Optical dating of Holocene sediments from a variety of geomorphic settings using single grains of quartz. *Geomorphology* 60 (3–4), 337–358.
- Orvin, A.K., 1934. *Geology of the Kings Bay Region, Spitsbergen*. Norges Svalbard- og Ishavsundersøkelser, Oslo.
- Praharaj, T., Swain, S.P., Powell, M.A., Hart, B.R., Tripathy, S., 2002. Delineation of groundwater contamination around an ash pond: geochemical and GIS approach. *Environment International* 27 (8), 631–638.
- Prescott, J.R., Hutton, J.T., 1994. Cosmic ray contributions to dose rates for luminescence and ESR dating: large depths and long-term time variations. *Radiation Measurements* 23, 497–500.
- Pusch, R., 1973. Densitet, vattenhalt och portal. In: Steen, B. (Ed.), *Byggeforskningens Informationsblad*, 5. Svenska Geotekniska Föreningen, Stockholm, 27 p. In Swedish.
- Rhodes, E.J., 2000. Observations of thermal transfer OSL signals in glacial quartz. *Radiation Measurements* 32 (5–6), 595–602.
- Rhodes, E.J., Pownall, L., 1994. Zeroing of the OSL signal in quartz from young glaciofluvial sediments. *Radiation Measurements* 23 (2–3), 581–585.
- Rink, W.J., 1997. Electron spin resonance (ESR) dating and ESR applications in quaternary science and archaeometry. *Radiation Measurements* 27 (5–6), 975–1025.
- Rose, N.L., Rose, C.L., Boyle, J.F., Appleby, P.G., 2004. Lake-sediment evidence for local and remote sources of atmospherically deposited pollutants on Svalbard. *Journal of Paleolimnology* 31 (4), 499–513.
- Schellmann, G., Radtke, U., 1997. Electron spin resonance (ESR) techniques applied to mollusc shells from South America (Chile, Argentina) and implications for palaeo sea-level curve. *Quaternary Science Reviews* 16 (3–5), 465–475.
- Sulerzhitsky, L.D., 1998. Mikrobnoe zagryaniye organicheskogo veshchestva iz vechnoy merzloty, nablyudaemoe pri radiouglerodnom datirovanii. *Kriosfera Zemli* 2 (1), 76–80 (In Russian).
- Svendsen, J.I., Alexanderson, H., Astakhov, V.I., Demidov, I., Dowdeswell, J.A., Funder, S., Gataullin, V., Henriksen, M., Hjort, C., Houmark-Nielsen, M., Hubberten, H.W., Ingólfsson, Ó., Jakobsson, M., Kjær, K.H., Larsen, E., Lokrantz, H., Lunikka, J.P., Lyså, A., Mangerud, J., Matiouchkov, A., Murray, A., Möller, P., Niessen, F., Nikolskaya, O., Polyak, L., Saarnisto, M., Siegert, C., Siegert, M.J., Spielhagen, R.F., Stein, R., 2004. Late Quaternary ice sheet history of northern Eurasia. *Quaternary Science Reviews* 23 (11–13), 1229–1271.
- Svensson, J., 2009. *Beach Processes and Recent Sea-level Changes at Tönsneset, Kongsfjorden, Northwestern Spitsbergen*. Department of Physical Geography and Quaternary Geology, Stockholm University. Bachelor Thesis KG2, 23 p.
- Troitsky, L., Punning, J.-M., Hütt, G., Rajamäe, R., 1979. Pleistocene glaciology of Spitsbergen. *Boreas* 8, 401–407.
- van Calsteren, P., Thomas, L., 2006. Uranium-series dating applications in natural environmental science. *Earth-Science Reviews* 75 (1–4), 155–175.
- Waelbroeck, C., Labeyrie, L., Michel, E., Duplessy, J.C., McManus, J.F., Lambeck, K., Balbon, E., Labracherie, M., 2002. Sea-level and deep water temperature changes derived from benthic foraminifera isotopic records. *Quaternary Science Reviews* 21 (1–3), 295–305.